Interacting scenarios with dynamical dark energy: Observational constraints and alleviation of the H_0 tension

Supriya Pan,[1,*] Weiqiang Yang,[2,†] Eleonora Di Valentino,[3,‡] Emmanuel N. Saridakis,[4,5,6,§] and Subenoy Chakraborty[7,‖]

[1]*Department of Mathematics, Presidency University, 86/1 College Street, Kolkata 700073, India*
[2]*Department of Physics, Liaoning Normal University, Dalian 116029, P. R. China*
[3]*Jodrell Bank Center for Astrophysics, School of Physics and Astronomy, University of Manchester, Oxford Road, Manchester M13 9PL, United Kingdom*
[4]*Department of Physics, National Technical University of Athens, Zografou Campus GR 157 73 Athens, Greece*
[5]*Department of Astronomy, School of Physical Sciences, University of Science and Technology of China, Hefei 230026, P.R. China*
[6]*National Observatory of Athens, Lofos Nymfon, 11852 Athens, Greece*
[7]*Department of Mathematics, Jadavpur University, Kolkata 700032, West Bengal, India*

(Received 21 July 2019; published 14 November 2019)

We investigate interacting scenarios that belong to a wider class, since they include a dynamical dark energy component whose equation of state follows various one-parameter parametrizations. We confront them with the latest observational data from the cosmic microwave background, the joint light-curve sample from type Ia supernovae, baryon acoustic oscillations, Hubble parameter measurements from cosmic chronometers (CC), and a Gaussian prior on the Hubble parameter H_0. In all examined scenarios we find a nonzero interaction; nevertheless, the noninteracting case is allowed within 2σ. Concerning the current value of the dark energy equation of state for all combinations of data sets, it always lies in the phantom regime at more than 2–3 standard deviations. Finally, for all interacting models, independently of the combination of data sets considered, the estimated values of the present Hubble parameter H_0 are greater compared to the ΛCDM-based *Planck* estimate and close to the local measurements, thus alleviating the H_0 tension.

DOI: 10.1103/PhysRevD.100.103520

I. INTRODUCTION

It has been 20 years since the detection of the late-time Universe acceleration, and—despite the accumulation of a huge amount of data—many are still looking for the actual underlying theory that explains it. In general, there are two widely accepted approaches that could accommodate it. The first one is the introduction of some hypothetical dark energy fluid [1] in the context of Einstein's gravitational theory. The second one is to consider modified or alternative gravitational theories where the extra geometrical terms may reproduce the effects of dark energy [2–4].

On the other hand, a mutual interaction between the dark matter and dark energy sectors was initially introduced in order to investigate the cosmological constant problem [5]. However, later on it was found that it could also alleviate the cosmic coincidence problem in a natural way [6–11], and this led to many investigations of interacting cosmology [12–61] (see also Refs. [62,63] for recent reviews on interacting dark matter–dark energy scenarios). An additional advantage of interacting scenarios is the easy realization of the phantom-divide crossing without theoretical ambiguities [64–66]. Finally, interacting scenarios prove to be efficient at alleviating the two known tensions of modern cosmology, namely, those of H_0 [67–95], and σ_8 [90,96–98].

Despite the extended investigation of interacting scenarios, the form of the interaction function remains unknown. Thus, in general one considers phenomenological models for the interaction form and explores the cosmological dynamics by confronting it with observational data. The complication in the above procedure, which is not usually taken into account, is that in principle apart from the unknown interaction form there is also an ambiguity in the dark-energy equation-of-state parameter. Hence, in the present work we are interested in performing a systematic comparison of interacting dark energy scenarios, considering all well-studied parametrizations for the dark-energy equation-of-state parameter. Only such a complete and

*supriya.maths@presiuniv.ac.in
†d11102004@163.com
‡eleonora.divalentino@manchester.ac.uk
§msaridak@phys.uoa.gr
‖schakraborty@math.jdvu.ac.in

consistent analysis can extract safe results about the observational validity of the examined scenarios.

We consider interacting scenarios in which the dark energy equation of state is parametrized with forms that include one free parameter. Such one-parameter models are more economical compared to two-parameter models; moreover, it was recently found that these one-parameter dynamical dark-energy parametrizations are very efficient at alleviating the H_0 tension in the simple noninteracting framework [83]. This motivates us to consider a wider picture in which the interaction should also be allowed, and to check whether the H_0 tension is still alleviated, since it has been argued that the allowance of a nongravitational interaction between dark matter and dark energy naturally increases the error bars on H_0 (due to the existing correlation between H_0 and the coupling parameter of the interaction models) and consequently alleviates the corresponding tension [69,70,79,81]. Thus, the present essentially work aims to investigate whether the release of H_0 tension discussed in Ref. [83] is influenced by the presence of an interaction between dark matter and dark energy.

The work is organized as follows. In Sec. II we describe the basic equations for any interacting dark energy model at the background and perturbative levels. Additionally, we present various one-parameter w_x parametrizations. Section III deals with the observational data that we consider in this work. In Sec. IV we describe the main observational results extracted for all of the examined scenarios. In Sec. V we compute the Bayesian evidences of the models with respect to the reference ΛCDM paradigm. Finally, in Sec. VI we conclude the present work with a brief summary of our findings.

II. COSMOLOGICAL EQUATIONS IN INTERACTING SCENARIOS

The Universe is well described by the homogeneous and isotropic Friedman-Lemaître-Robertson-Walker (FLRW) line element given by

TABLE I. Priors imposed on various free parameters of the interacting scenarios during the statistical analysis.

Parameter	Prior
$\Omega_b h^2$	[0.005, 0.1]
$\Omega_c h^2$	[0.01, 0.99]
τ	[0.01, 0.8]
n_s	[0.5, 1.5]
$\log[10^{10}A_s]$	[2.4, 4]
$100\theta_{\rm MC}$	[0.5, 10]
w_0	$[-2, 0]$
ξ	[0, 2]

TABLE II. 68% and 95% confidence level constraints on the interacting scenario IDE1 with the dark energy equation of state $w_x(a) = w_0 a[1 - \log(a)]$ (Model I) for various observational data sets. Here, Ω_{m0} is the present value of the total matter density parameter $\Omega_m = \Omega_b + \Omega_c$, and H_0 is in units of km/sec/Mpc.

Parameters	CMB	CMB + BAO	CMB + BAO + JLA	CMB + BAO + JLA + CC	CMB + R19	CMB + BAO + R19
$\Omega_c h^2$	$0.1209^{+0.0015+0.0038}_{-0.0020-0.0035}$	$0.1194^{+0.0013+0.0025}_{-0.0013-0.0025}$	$0.1187^{+0.0012+0.0023}_{-0.0012-0.0022}$	$0.1187^{+0.0012+0.0025}_{-0.0012-0.0025}$	$0.1202^{+0.0015+0.0028}_{-0.0016-0.0027}$	$0.1198^{+0.0012+0.0024}_{-0.0012-0.0024}$
$\Omega_b h^2$	$0.02220^{+0.00016+0.00031}_{-0.00015-0.00031}$	$0.02223^{+0.00016+0.00028}_{-0.00015-0.00029}$	$0.02226^{+0.00014+0.00028}_{-0.00014-0.00027}$	$0.02226^{+0.00014+0.00028}_{-0.00014-0.00028}$	$0.02219^{+0.00015+0.00028}_{-0.00015-0.00028}$	$0.02222^{+0.00015+0.00030}_{-0.00016-0.00031}$
$100\theta_{\rm MC}$	$1.04036^{+0.00037+0.00065}_{-0.00031-0.00070}$	$1.04049^{+0.00032+0.00063}_{-0.00032-0.00065}$	$1.04058^{+0.00030+0.00060}_{-0.00030-0.00058}$	$1.04059^{+0.00029+0.00059}_{-0.00031-0.00060}$	$1.04040^{+0.00035+0.00056}_{-0.00032-0.00060}$	$1.04044^{+0.00033+0.00062}_{-0.00033-0.00060}$
τ	$0.080^{+0.018+0.035}_{-0.018-0.035}$	$0.086^{+0.018+0.036}_{-0.018-0.036}$	$0.092^{+0.017+0.034}_{-0.018-0.034}$	$0.092^{+0.018+0.033}_{-0.017-0.034}$	$0.081^{+0.017+0.034}_{-0.019-0.032}$	$0.082^{+0.018+0.037}_{-0.018-0.037}$
n_s	$0.9734^{+0.0044+0.0081}_{-0.0044-0.0082}$	$0.9748^{+0.0042+0.0084}_{-0.0041-0.0082}$	$0.9764^{+0.0041+0.0081}_{-0.0040-0.0079}$	$0.9766^{+0.0041+0.0088}_{-0.0042-0.0083}$	$0.9734^{+0.0047+0.0082}_{-0.0047-0.0083}$	$0.9739^{+0.0040+0.0083}_{-0.0041-0.0077}$
$\ln(10^{10}A_s)$	$3.103^{+0.034+0.067}_{-0.034-0.067}$	$3.114^{+0.037+0.070}_{-0.034-0.069}$	$3.124^{+0.034+0.067}_{-0.035-0.065}$	$3.124^{+0.036+0.065}_{-0.033-0.065}$	$3.107^{+0.033+0.068}_{-0.037-0.068}$	$3.108^{+0.035+0.072}_{-0.034-0.072}$
w_0	$<-1.30<-1.07$	$-1.207^{+0.058+0.11}_{-0.054-0.11}$	$-1.137^{+0.037+0.074}_{-0.037-0.073}$	$-1.138^{+0.041+0.082}_{-0.040-0.085}$	$-1.306^{+0.053+0.09}_{-0.046-0.10}$	$-1.263^{+0.041+0.089}_{-0.040-0.088}$
ξ	$<0.0068 < 0.014$	$<0.0047 < 0.0071$	$0.0030^{+0.0019}_{-0.0020} < 0.0058$	$0.0031^{+0.0019}_{-0.0021} < 0.0059$	$<0.0061 < 0.0088$	$<0.0054 < 0.0080$
Ω_{m0}	$0.231^{+0.077+0.109}_{-0.081-0.098}$	$0.283^{+0.011+0.022}_{-0.011-0.022}$	$0.297^{+0.0087+0.0171}_{-0.0088-0.0169}$	$0.296^{+0.0088+0.0175}_{-0.0086-0.0176}$	$0.2632^{+0.0095+0.020}_{-0.0095-0.020}$	$0.271^{+0.0077+0.016}_{-0.0074-0.016}$
σ_8	$0.932^{+0.087+0.144}_{-0.090-0.143}$	$0.855^{+0.021+0.040}_{-0.021-0.038}$	$0.835^{+0.018+0.034}_{-0.017-0.034}$	$0.836^{+0.017+0.035}_{-0.017-0.033}$	$0.882^{+0.018+0.034}_{-0.020-0.033}$	$0.870^{+0.019+0.032}_{-0.017-0.035}$
H_0	81^{+13+17}_{-14-16}	$71.0^{+1.5+2.9}_{-1.5-3.0}$	$69.1^{+1.0+2.0}_{-1.0-2.0}$	$69.2^{+1.0+2.1}_{-1.1-2.1}$	$73.8^{+1.2+3.0}_{-1.5-2.6}$	$72.6^{+1.0+2.2}_{-1.0-2.0}$
S_8	$0.820^{+0.038+0.061}_{-0.045-0.08}$	$0.824^{+0.019+0.035}_{-0.017-0.055}$	$0.823^{+0.020+0.036}_{-0.017-0.057}$	$0.825^{+0.017+0.034}_{-0.015-0.051}$	$0.826^{+0.026+0.031}_{-0.016-0.030}$	$0.826^{+0.015+0.030}_{-0.016-0.030}$

$$ds^2 = -dt^2 + a^2(t)\left[\frac{dr^2}{1-Kr^2} + (d\theta^2 + \sin^2\theta d\phi^2)\right], \quad (1)$$

where $a(t)$ is the expansion scale factor and $K = 0, -1, +1$ correspond to flat, open, and closed spatial geometry, respectively. Since observations imply near spatial flatness, we shall restrict ourselves to $K = 0$ throughout this work.

The total matter content of the Universe consists of radiation, baryons, pressureless dark matter, and a dark energy fluid (which may be a real fluid or an effective one arising from modified gravity). Moreover, we allow the dark matter and dark energy to have a mutual (nongravitational) interaction, while the remaining two fluids follow the usual conservation laws. Hence, the Friedmann equation is given by

$$H^2 = \frac{8\pi G}{3}(\rho_r + \rho_b + \rho_c + \rho_x), \quad (2)$$

in which $H \equiv \dot{a}/a$ is the Hubble rate, and ρ_i is the energy density of the ith fluid sector (with $i = r$ for radiation, $i = b$ for baryons, $i = c$ for cold or pressureless dark matter, and $i = x$ for dark energy). The conservation equation of the total fluid $\rho_{\rm tot} = \rho_r + \rho_b + \rho_c + \rho_x$ is given by

$$\dot{\rho}_{\rm tot} + 3H(\rho_{\rm tot} + p_{\rm tot}) = 0, \quad (3)$$

where $p_{\rm tot}$ is the total pressure of the fluids, defined as $p_{\rm tot} = p_r + p_b + p_c + p_x$. Since radiation and baryons satisfy their own conservation equations, namely, $\dot{\rho}_b + 3H\rho_b = 0$ and $\dot{\rho}_r + 4H\rho_r = 0$, then the conservation equation for the total fluid (3) gives rise to

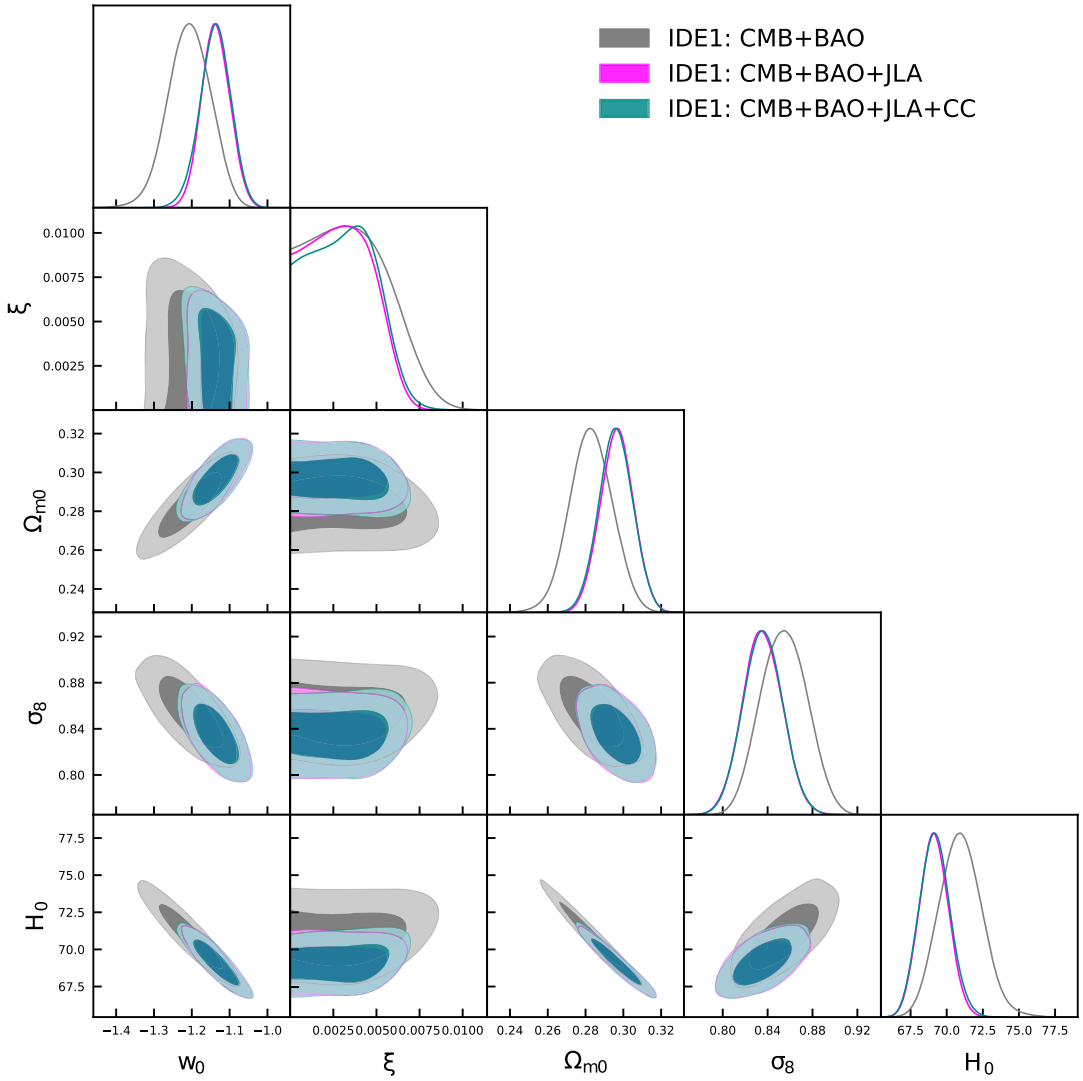

FIG. 1. The 68% and 95% C.L. contour plots between various combinations of the model parameters of scenario IDE1, using different observational astronomical data sets. Additionally, we display the one-dimensional marginalized posterior distributions of some free parameters.

$$\dot{\rho}_{\rm Dark} + 3H(p_{\rm Dark} + \rho_{\rm Dark}) = 0, \tag{4}$$

where $\rho_{\rm Dark} = \rho_c + \rho_x$ and $p_{\rm Dark} = p_c + p_x$.

In interacting cosmology one splits the conservation equation for the dark sector (4) into

$$\dot{\rho}_c + 3H\rho_c = -Q(t) \tag{5}$$

and

$$\dot{\rho}_x + 3H(1 + w_x)\rho_x = Q(t) \tag{6}$$

by introducing a new function $Q(t)$ that actually characterizes the rate of energy transfer between these dark fluids. Thus, whenever the interaction Q is prescribed, using the conservation equations (5)–(6) as well as the Friedmann equation (2), one can determine the dynamics of this interacting scenario.

Since the nature of both dark fluids is unknown, there is an ambiguity in the choice of the interaction function. Thus, in general one considers phenomenological choices for Q, and through observational confrontation arrives at the best interaction model. In the present work we will focus on a well-motivated interaction that induces stable perturbations [99]:

$$Q = 3\xi H(1 + w_x)\rho_x, \tag{7}$$

where ξ is the coupling parameter characterizing the interaction strength.

Let us briefly describe the perturbation equations for an interacting dark energy model following Refs. [100–102]. The scalar perturbations of the FLRW metric read as

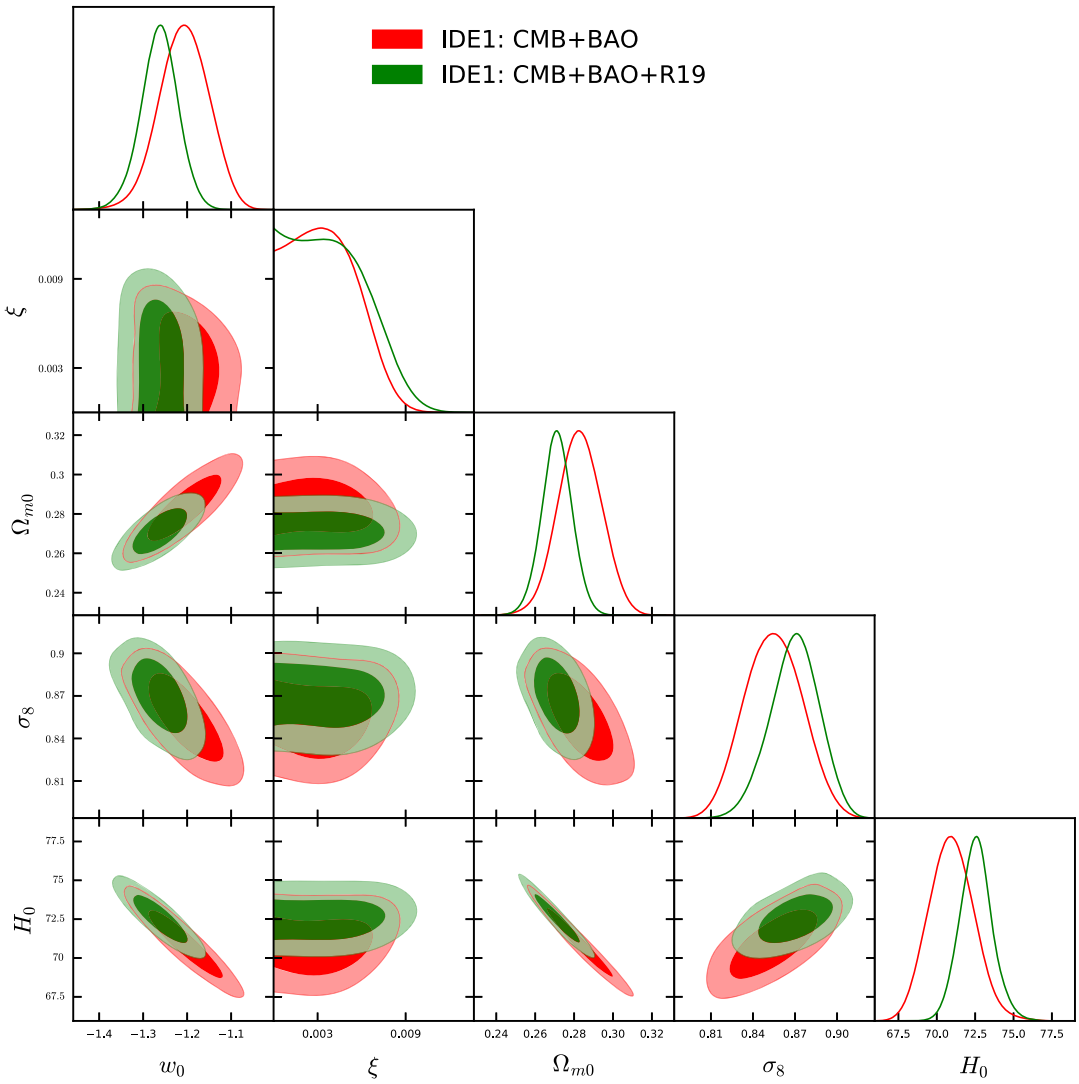

FIG. 2. The 68% and 95% C.L. contour plots between various combinations of the model parameters of scenario IDE1 using only the CMB + BAO and CMB + BAO + R19 data sets, and the corresponding one-dimensional marginalized posterior distributions.

$$ds^2 = a^2(\tau)[-(1+2\phi)d\tau^2 + 2\partial_i B d\tau dx^i + ((1-2\psi)\delta_{ij} + 2\partial_i\partial_j E)dx^i dx^j], \quad (8)$$

where τ is the conformal time and ϕ, B, ψ, and E are the gauge-dependent scalar perturbation quantities. Additionally, for an interacting universe the conservation equations become [103–105]

$$\nabla_\nu T^{\mu\nu}_A = Q^\mu_A, \qquad \sum_A Q^\mu_A = 0, \quad (9)$$

where A is used to represent either pressureless dark matter ($A = c$) or dark energy ($A = x$). Here, the quantity Q^μ_A is

$$Q^\mu_A = (Q_A + \delta Q_A)u^\mu + a^{-1}(0, \partial^i f_A) \quad (10)$$

relative to the four-velocity u^μ, in which Q_A presents the background energy transfer (i.e., $Q_A = Q$) and f_A is the momentum transfer potential. Following earlier works [103–105], we restrict ourselves to the simplest possibility, i.e., we assume that the momentum transfer potential is zero in the rest frame of the dark matter, from which one can derive that $k^2 f_A = Q_A(\theta - \theta_c)$ (where k is the wave number, $\theta = \theta^\mu_\mu$ is the volume expansion scalar of the total fluid, and θ_c is the volume expansion scalar for the cold dark matter fluid).

We proceed by applying the synchronous gauge to derive the perturbation equations for the interacting scenarios. Thus, in the synchronous gauge we have $\phi = B = 0$, $\psi = \eta$, and $k^2 E = -h/2 - 3\eta$ (where h and η are the metric perturbations; see Ref. [101] for details). Additionally, we assume the absence of an anisotropic stress, and we define the density perturbations for the fluid A as $\delta_A = \delta\rho_A/\rho_A$. The resulting perturbation equations become

$$\delta'_x = -(1+w_x)\left(\theta_x + \frac{h'}{2}\right) - 3\mathcal{H}w'_x\frac{\theta_x}{k^2} - 3\mathcal{H}(c^2_{sx} - w_x)\left[\delta_x + 3\mathcal{H}(1+w_x)\frac{\theta_x}{k^2}\right] + \frac{aQ}{\rho_x}\left[-\delta_x + \frac{\delta Q}{Q} + 3\mathcal{H}(c^2_{sx} - w_x)\frac{\theta_x}{k^2}\right], \quad (11)$$

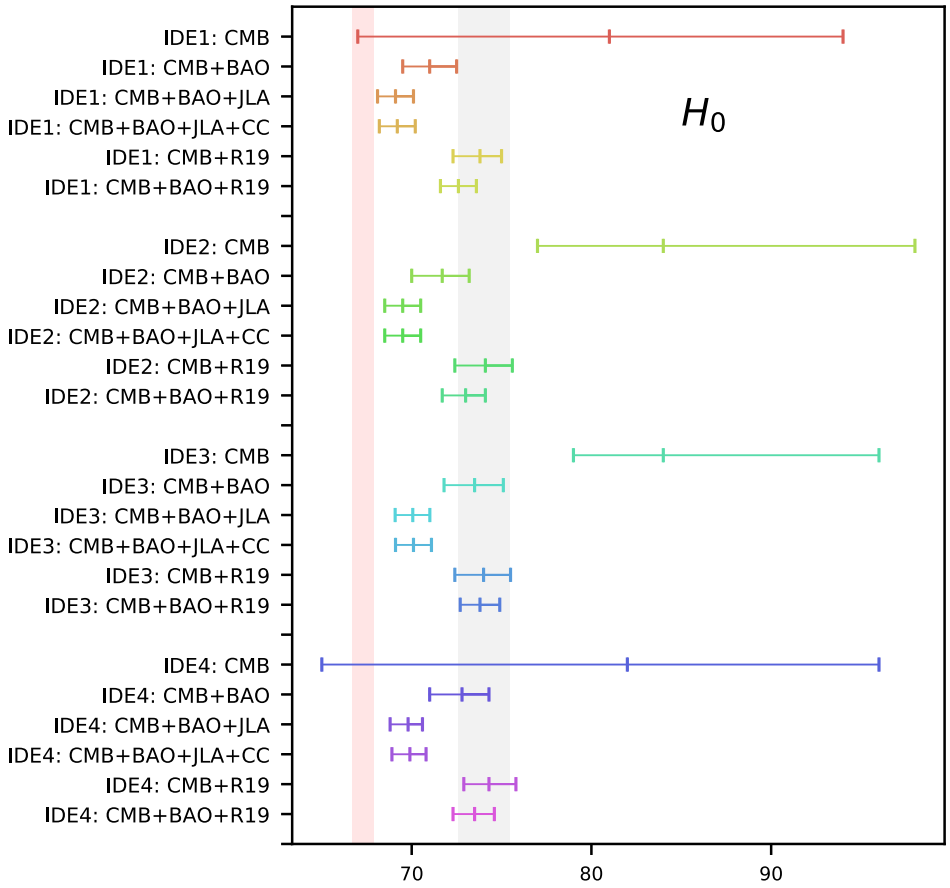

FIG. 3. Whisker plot with the 68% C.L. constraints on the Hubble constant for all interacting models and all combinations of data sets considered in this work. The grey vertical band corresponds to the R19 value for the Hubble constant H_0, as measured by SH0ES in Ref. [113], and the red vertical band is the estimate from the *Planck* 2018 release [116].

$$\theta_x' = -\mathcal{H}(1-3c_{sx}^2)\theta_x + \frac{c_{sx}^2}{(1+w_x)}k^2\delta_x + \frac{aQ}{\rho_x}\left[\frac{\theta_c-(1+c_{sx}^2)\theta_x}{1+w_x}\right], \tag{12}$$

$$\delta_c' = -\left(\theta_c + \frac{h'}{2}\right) + \frac{aQ}{\rho_c}\left(\delta_c - \frac{\delta Q}{Q}\right), \tag{13}$$

$$\theta_c' = -\mathcal{H}\theta_c, \tag{14}$$

where $\mathcal{H} = aH$ is the conformal Hubble rate, and in Eqs. (11), (12), and (13) the factor $\delta Q/Q$ incorporates the perturbations for the Hubble rate δH. We mention that by using δH one can easily find the gauge-invariant perturbation equations [17].

We close this section by introducing the w_x parametrizations that have only one free parameter w_0, namely, the present value of the dark energy equation of state [83]:

$$\text{Model I:}\ w_x(a) = w_0 a[1-\log(a)], \tag{15}$$

$$\text{Model II:}\ w_x(a) = w_0 a\exp(1-a), \tag{16}$$

$$\text{Model III:}\ w_x(a) = w_0 a[1+\sin(1-a)], \tag{17}$$

$$\text{Model IV:}\ w_x(a) = w_0 a[1+\arcsin(1-a)]. \tag{18}$$

Thus, in summary we consider the interaction model (7) with four different dark energy equations of state given in Eqs. (15)–(18). From now on we denote the interaction model (7) with w_x of Eq. (15) as IDE1, the interaction model (7) with Eq. (16) as IDE2, interaction model (7) with Eq. (17) as IDE3, and finally the interaction model (7) with Eq. (18) as IDE4.

III. OBSERVATIONAL DATA

In this section we describe the observational data that we use to investigate the interacting dark energy models and provide a brief description of the methodology.

(1) The data from cosmic microwave background (CMB) observations are very powerful for analyzing cosmological models. Here we use the high-ℓ temperature and polarization as well as the low-ℓ temperature and polarization 2015 CMB angular power spectra from the *Planck* experiment (*Planck* TT, TE, EE + lowTEB) [106,107].

(2) We include the joint light-curve analysis (JLA) sample from type Ia supernovae data [108].

(3) We use the baryon acoustic oscillation (BAO) distance measurements from Refs. [109–111].

(4) We consider the measurements of the Hubble parameter at various redshifts using cosmic chronometers (CCs) [112].

TABLE III. 68% and 95% confidence-level constraints on the interacting scenario IDE2 with the dark energy equation of state $w_x(a) = w_0 a\exp(1-a)$ (Model II) for various observational data sets. Here Ω_{m0} is the present value of the total matter density parameter $\Omega_m = \Omega_b + \Omega_c$, and H_0 is in units of km/sec/Mpc.

Parameters	CMB	CMB + BAO	CMB + BAO + JLA	CMB + BAO + JLA + CC	CMB + R19	CMB + BAO + R19
$\Omega_c h^2$	$0.1214^{+0.0017+0.0042}_{-0.0022-0.0040}$	$0.1197^{+0.0012+0.0025}_{-0.0012-0.0024}$	$0.1191^{+0.0011+0.0022}_{-0.0011-0.0023}$	$0.1191^{+0.0012+0.0024}_{-0.0012-0.0024}$	$0.12061377^{+0.0015+0.0029}_{-0.0014-0.0039}$	$0.1199^{+0.0012+0.0024}_{-0.0013-0.0023}$
$\Omega_b h^2$	$0.02218^{+0.00016+0.00032}_{-0.00016-0.00034}$	$0.02221^{+0.00014+0.00029}_{-0.00015-0.00026}$	$0.02222^{+0.00014+0.00027}_{-0.00014-0.00027}$	$0.02223^{+0.00014+0.00027}_{-0.00013-0.00026}$	$0.02215^{+0.00014+0.00027}_{-0.00013-0.00026}$	$0.02220^{+0.00014+0.00029}_{-0.00016-0.00028}$
$100\theta_{\rm MC}$	$1.04034^{+0.00035+0.00071}_{-0.00034-0.00072}$	$1.04045^{+0.00031+0.00058}_{-0.00030-0.00060}$	$1.04050^{+0.00034+0.00058}_{-0.00031-0.00060}$	$1.04051^{+0.00032+0.00066}_{-0.00032-0.00065}$	$1.04036^{+0.00034+0.00068}_{-0.00034-0.00073}$	$1.04042^{+0.00030+0.00060}_{-0.00030-0.00060}$
τ	$0.079^{+0.018+0.034}_{-0.018-0.035}$	$0.088^{+0.018+0.034}_{-0.018-0.035}$	$0.095^{+0.016+0.032}_{-0.017-0.033}$	$0.094^{+0.018+0.033}_{-0.017-0.033}$	$0.082^{+0.017+0.033}_{-0.016-0.036}$	$0.086^{+0.017+0.033}_{-0.017-0.033}$
n_s	$0.9729^{+0.0045+0.0089}_{-0.0045-0.0092}$	$0.9748^{+0.0042+0.0084}_{-0.0043-0.0084}$	$0.9762^{+0.0042+0.0082}_{-0.0042-0.0081}$	$0.9764^{+0.0042+0.0079}_{-0.0045-0.0076}$	$0.9723^{+0.0051+0.0098}_{-0.0049-0.0094}$	$0.9741^{+0.0040+0.0084}_{-0.0040-0.0084}$
$\ln(10^{10}A_s)$	$3.103^{+0.035+0.066}_{-0.035-0.070}$	$3.119^{+0.035+0.066}_{-0.034-0.068}$	$3.131^{+0.032+0.066}_{-0.032-0.064}$	$3.129^{+0.033+0.065}_{-0.034-0.067}$	$3.108^{+0.034+0.063}_{-0.031-0.072}$	$3.115^{+0.035+0.065}_{-0.033-0.064}$
w_0	$< -1.53 < -1.08$	$-1.249^{+0.064+0.12}_{-0.055-0.12}$	$-1.166^{+0.038+0.072}_{-0.038-0.074}$	$-1.168^{+0.041+0.075}_{-0.034-0.081}$	$-1.341^{+0.058+0.09}_{-0.047-0.11}$	$-1.292^{+0.051+0.083}_{-0.042-0.089}$
ξ	$<0.0071 < 0.015$	$0.0024^{+0.0015}_{-0.0016} < 0.0047$	$<0.0027 < 0.0038$	$0.0021^{+0.0014}_{-0.0013} < 0.0039$	$0.0024^{+0.0009}_{-0.0021} < 0.0053$	$0.0027^{+0.0016}_{-0.0017} < 0.0051$
Ω_{m0}	$0.212^{+0.023+0.132}_{-0.071-0.085}$	$0.277^{+0.012+0.022}_{-0.011-0.023}$	$0.295^{+0.0086+0.017}_{-0.0085-0.018}$	$0.294^{+0.0085+0.018}_{-0.0086-0.018}$	$0.261^{+0.011+0.022}_{-0.011-0.022}$	$0.2683^{+0.0076+0.016}_{-0.0081-0.016}$
σ_8	$0.956^{+0.100+0.123}_{-0.044-0.169}$	$0.859^{+0.022+0.043}_{-0.022-0.043}$	$0.835^{+0.017+0.032}_{-0.017-0.033}$	$0.835^{+0.018+0.037}_{-0.018-0.036}$	$0.886^{+0.020+0.037}_{-0.023-0.036}$	$0.872^{+0.020+0.038}_{-0.019-0.038}$
H_0	84^{+14+16}_{-7-21}	$71.7^{+1.5+3.3}_{-1.7-3.1}$	$69.5^{+1.0+2.0}_{-1.0-1.9}$	$69.5^{+1.0+2.0}_{-1.0-1.9}$	$74.1^{+1.5+2.9}_{-1.7-2.8}$	$73.0^{+1.1+2.2}_{-1.3-2.1}$
S_8	$0.811^{+0.045+0.069}_{-0.048-0.078}$	$0.817^{+0.020+0.038}_{-0.017-0.069}$	$0.820^{+0.020+0.037}_{-0.018-0.065}$	$0.819^{+0.020+0.036}_{-0.019-0.060}$	$0.826^{+0.017+0.034}_{-0.016-0.035}$	$0.824^{+0.016+0.030}_{-0.015-0.031}$

(5) We adopt a Gaussian prior on the Hubble constant (R19), $H_0 = 74.02 \pm 1.42$, as obtained by SH0ES [113].

In order to extract the observational constraints on the model parameters of the interaction scenarios, we use the efficient cosmological code COSMOMC [114,115], a Markov chain Monte Carlo package which (i) has a convergence diagnostic and (ii) supports the *Planck* 2015 likelihood code [107]. The dimension of the parameter space for all interaction scenarios is eight, where $\mathcal{P} \equiv \{\Omega_b h^2, \Omega_c h^2, 100\theta_{\rm MC}, \tau, w_0, \xi, n_s, \log[10^{10} A_S]\}$. Here $\Omega_b h^2$ is the physical baryon density, $\Omega_c h^2$ is the physical density of cold dark matter, $100\theta_{\rm MC}$ denotes the ratio of the sound horizon to the angular diameter distance, τ denotes the reionization optical depth, n_s is the scalar spectral index, A_S is the amplitude of the primordial scalar power spectrum, w_0 is the current value of the dark energy parameter, and ξ is the coupling parameter of the interaction. In Table I we summarize the flat priors on the model parameters during the statistical analysis.

IV. RESULTS AND IMPLICATIONS

In this section we extract the observational constraints on the present four interacting dark energy scenarios where dark energy has a time-dependent equation-of-state parameter. For all interacting scenarios we perform several analyses using the observational data described in Sec. III.

A. IDE1: Interacting dark energy with $w_x = w_0 a[1 - \log(a)]$

The summary of the observational constraints for this interaction scenario using different observational data sets

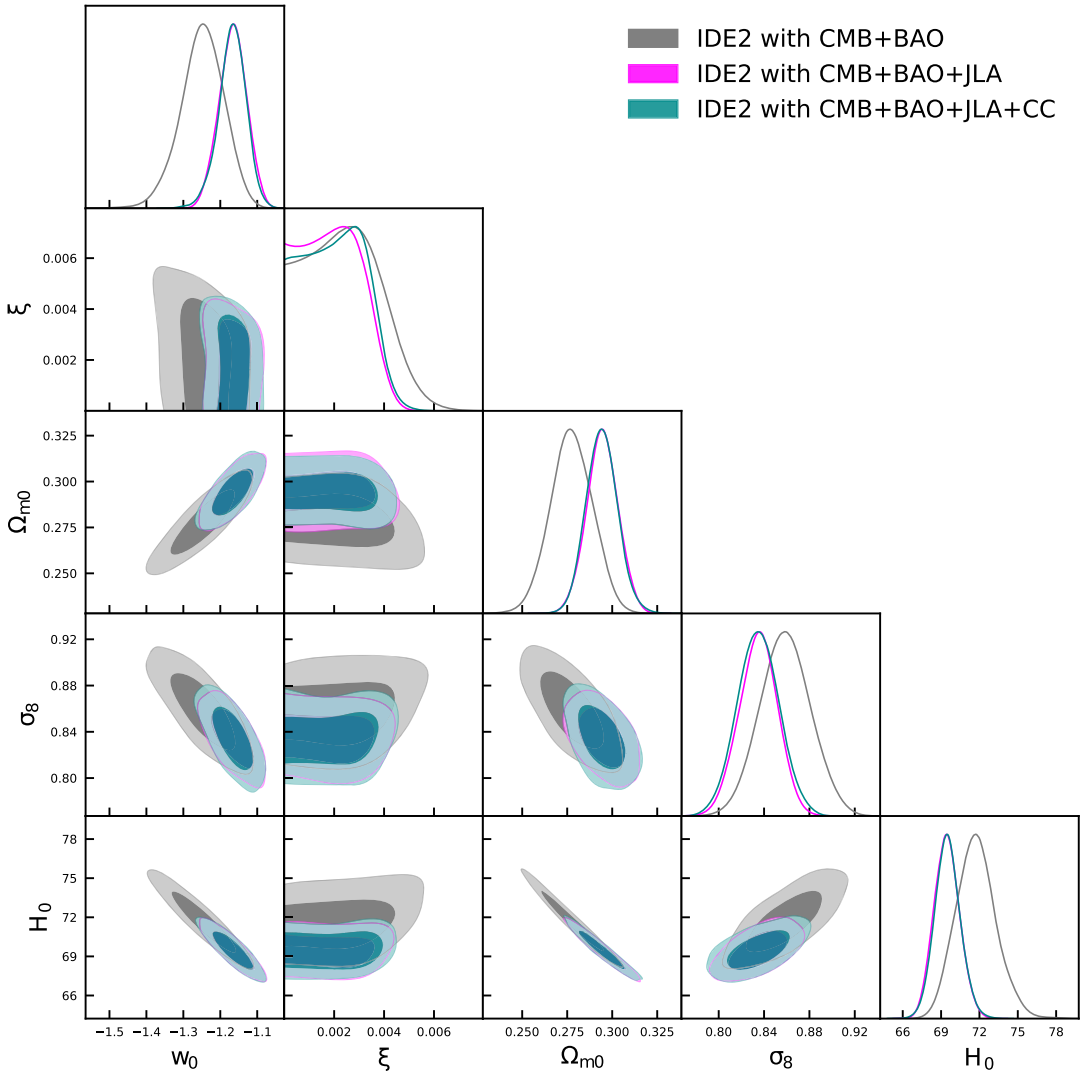

FIG. 4. The 68% and 95% C.L. contour plots between various combinations of the model parameters of scenario IDE2, using different observational astronomical data sets. Additionally, we display the one-dimensional marginalized posterior distributions of some of the free parameters.

is presented in Table II, while the two-dimensional (2D) contour plots and one-dimensional (1D) marginalized posterior distribution are shown in Figs. 1 and 2. We mention that in the figures we do not include the sole CMB case, since its parameter space is larger than the other data sets; however, we note that the qualitative features of the correlations between the parameters for the CMB-only case and other cases are similar. Moreover, we notice that the addition of CC to the CMB + BAO + JLA combination does not add extra constraining power, and hence the constraints from CMB + BAO + JLA and CMB + BAO + JLA + CC are actually the same in the fourth and fifth columns of Table II.

From the results we observe that for both CMB and CMB + BAO $\xi = 0$ is consistent within the 68% C.L. After the addition of JLA and JLA + CC to the combined data set CMB + BAO, we find that an interaction of about $\xi = 0.003 \pm 0.002$ is suggested at the 68% C.L. In addition, if we combine CMB with R19 (we can safely do this since the tension on H_0 is less than 2σ, as we can see in Fig. 3) we find an improved constraint (statistically very mild) that is always in agreement with $\xi = 0$, while combining CMB + BAO + R19 gives slightly relaxed constraints Therefore, we conclude that for CMB + BAO + JLA, CMB + BAO + JLA + CC, CMB + R19, and CMB + BAO + R19, $\xi \neq 0$ at 1σ; however, within the 95% C.L., ξ is consistent with zero.

For all combinations of data sets the current value of the dark energy equation of state w_0 always lies in the phantom regime at more than 2–3 standard deviations. If we compare these results with those without an interaction obtained in Ref. [83], we see that they are perfectly in agreement and very robust, even in those cases where an interaction different from zero is favored.

Regarding the estimated values of Ω_{m0}, one can clearly see that for the CMB-only case, Ω_{m0} is really small

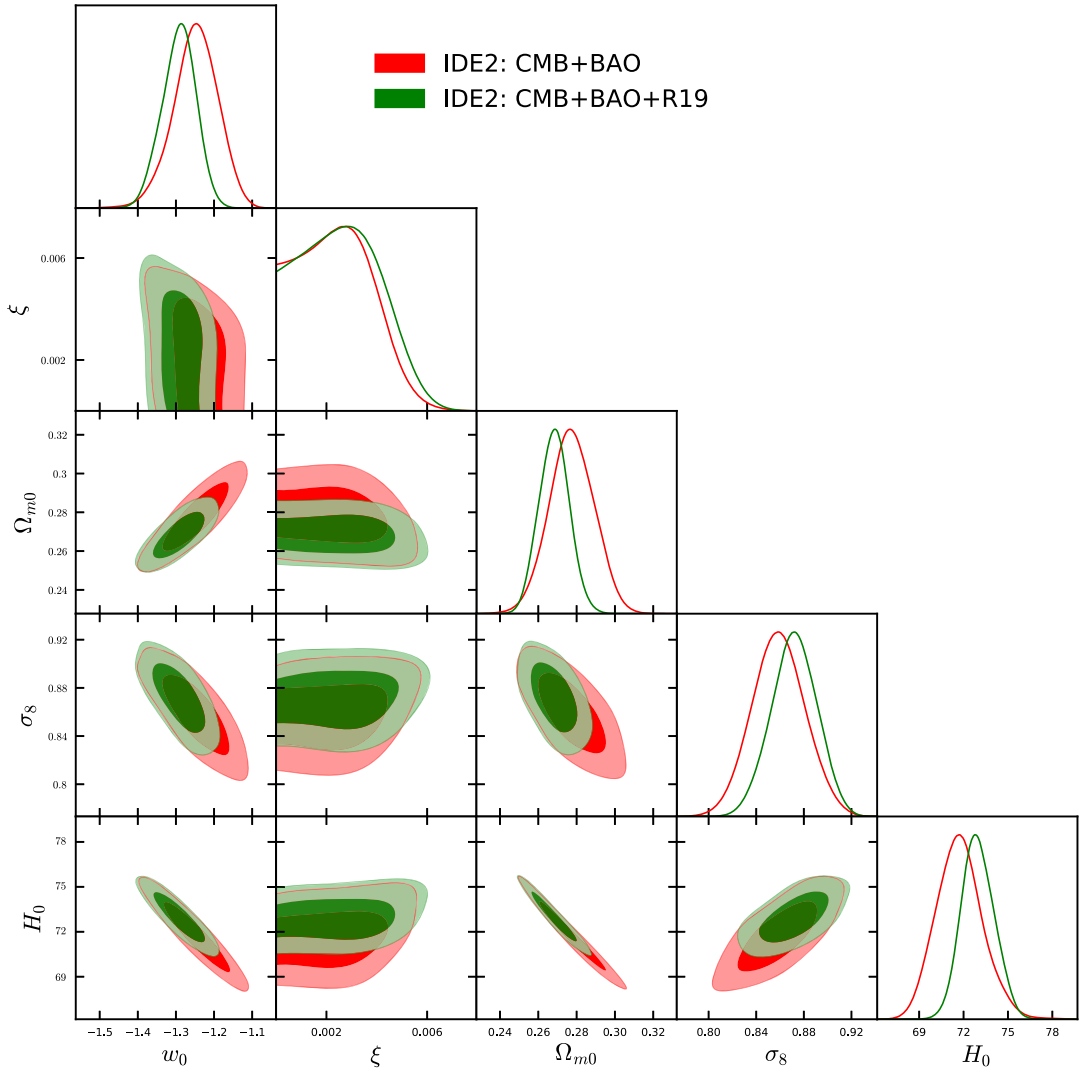

FIG. 5. The 68% and 95% C.L. contour plots between various combinations of the model parameters of scenario IDE2 using only the CMB + BAO and CMB + BAO + R19 data sets, and the corresponding one-dimensional marginalized posterior distributions.

compared to the *Planck* estimate [117]. This is due to the geometrical degeneracy existing between w_0, $\Omega_{m,0}$, and H_0. Since a phantom dark energy equation of state is preferred by the *Planck* data, the position of the peaks in the high-multipole damping tail will be shifted, and we need a lower value for the matter density and a higher Hubble constant to put them back in the measured position. When BAO data are added to the CMB data, the mean value of Ω_{m0} increases with reduced error bars because this data set fixes the matter density in the Universe very well. For this reason, all of the other data set combinations we considered have Ω_{m0} values greater than the CMB-only case, even if they are always lower than the *Planck* estimate [117].

Finally, concerning the estimation of H_0, we see that for CMB data alone it takes a very high mean value compared to the ΛCDM-based *Planck* estimate [116] and the error bars are quite large ($H_0 = 81^{+13}_{-14}$ at 68% C.L. for CMB data alone). This is an implication of the strong anticorrelation between w_0 and H_0. However, when the BAO data are added to CMB, the error bars on H_0 are significantly decreased and its estimated mean value shifts toward a lower value ($H_0 = 71.0 \pm 1.5$ at 68% C.L. for CMB + BAO), i.e., it is in perfect agreement with the direct measurements [113,118,119] within 2σ. The addition of JLA (or JLA + CC) to CMB + BAO further decreases the error bars on H_0 and shifts its value lower, increasing the H_0 tension, but it is still less than 3σ.

B. IDE2: Interacting dark energy with $w_x(a) = w_0 a \exp(1-a)$

The observational summary for this interaction scenario is displayed in Table III, while the 2D contour plots and 1D parameter distributions are shown in Figs. 4 and 5. From the analyses we deduce that for CMB data alone the noninteracting case $\xi = 0$ is consistent within 68% C.L.; however, when BAO data are added to CMB then an indication of an interaction is found at more than 68% C.L. Surprisingly, when JLA data are added to the previous data set CMB + BAO, we again find that $\xi = 0$ consistent within 68% C.L. Moreover, for the remaining data sets the indication of an interaction is still present at more than 1σ. We note that due to the addition of R19 to CMB and CMB + BAO data, slight improvements in the coupling parameter ξ are observed, although such improvements are statistically very mild. In fact, R19 sets a lower bound on ξ for both CMB+R19 and CMB + BAO + R19. The reason is that the addition of R19 to CMB and CMB + BAO breaks the degeneracies between H_0 and other cosmological parameters.

Concerning the dark energy equation-of-state parameter at present, for all of the data sets a phantom value $w_0 < -1$ is always supported for more than 95% C.L. Hence, in

TABLE IV. 68% and 95% confidence level constraints on the interacting scenario IDE3 with the dark energy equation of state $w_x(a) = w_0 a[1 + \sin(1-a)]$ (Model III) for various observational data sets. Here Ω_{m0} is the present value of the total matter density parameter $\Omega_m = \Omega_b + \Omega_c$, and H_0 is in units of km/sec/Mpc.

Parameters	CMB	CMB + BAO	CMB + BAO + JLA	CMB + BAO + JLA + CC	CMB + R19	CMB + BAO + R19
$\Omega_c h^2$	$0.1211^{+0.0015+0.0031}_{-0.0015-0.0031}$	$0.1202^{+0.0011+0.0025}_{-0.0013-0.0023}$	$0.1196^{+0.0011+0.0022}_{-0.0012-0.0023}$	$0.1196^{+0.0011+0.0022}_{-0.0012-0.0021}$	$0.1212^{+0.0014+0.0030}_{-0.0016-0.0029}$	$0.1203^{+0.0012+0.0024}_{-0.0013-0.0023}$
$\Omega_b h^2$	$0.02216^{+0.00019+0.00035}_{-0.00016-0.00037}$	$0.02216^{+0.00014+0.00027}_{-0.00014-0.00027}$	$0.02218^{+0.00015+0.00028}_{-0.00016-0.00028}$	$0.02218^{+0.00013+0.00026}_{-0.00013-0.00027}$	$0.02208^{+0.00016+0.00029}_{-0.00016-0.00030}$	$0.02216^{+0.00014+0.00027}_{-0.00014-0.00027}$
$100\theta_{\rm MC}$	$1.04033^{+0.00039+0.00066}_{-0.00035-0.00070}$	$1.04035^{+0.00033+0.00060}_{-0.00030-0.00062}$	$1.04043^{+0.00030+0.00058}_{-0.00030-0.00059}$	$1.04041^{+0.00030+0.00058}_{-0.00029-0.00056}$	$1.04019^{+0.00039+0.00066}_{-0.00036-0.00070}$	$1.04036^{+0.00033+0.00060}_{-0.00030-0.00063}$
τ	$0.079^{+0.017+0.035}_{-0.018-0.035}$	$0.089^{+0.019+0.034}_{-0.017-0.035}$	$0.098^{+0.018+0.036}_{-0.018-0.035}$	$0.098^{+0.017+0.034}_{-0.017-0.033}$	$0.083^{+0.020+0.037}_{-0.020-0.037}$	$0.089^{+0.019+0.033}_{-0.017-0.034}$
n_s	$0.9725^{+0.0046+0.0087}_{-0.0045-0.0086}$	$0.9740^{+0.0040+0.0076}_{-0.0040-0.0080}$	$0.9761^{+0.0042+0.0080}_{-0.0042-0.0080}$	$0.9764^{+0.0039+0.0077}_{-0.0040-0.0077}$	$0.9713^{+0.0044+0.0090}_{-0.0051-0.0082}$	$0.9739^{+0.0040+0.0076}_{-0.0040-0.0081}$
$\ln(10^{10}A_s)$	$3.102^{+0.033+0.068}_{-0.035-0.065}$	$3.120^{+0.037+0.064}_{-0.034-0.068}$	$3.135^{+0.034+0.069}_{-0.035-0.069}$	$3.136^{+0.032+0.065}_{-0.033-0.064}$	$3.111^{+0.040+0.067}_{-0.038-0.068}$	$3.120^{+0.033+0.063}_{-0.033-0.064}$
w_0	$< -1.61 < -1.17$	$-1.371^{+0.066+0.12}_{-0.058-0.12}$	$-1.246^{+0.040+0.065}_{-0.033-0.072}$	$-1.248^{+0.037+0.065}_{-0.035-0.070}$	$-1.406^{+0.051+0.093}_{-0.053-0.091}$	$-1.380^{+0.044+0.083}_{-0.044-0.084}$
ξ	$<0.0045 < 0.0080$	$0.0019^{+0.0011}_{-0.0012} < 0.0036$	$0.0015^{+0.0010}_{-0.0008} < 0.0027$	$0.0015^{+0.0011}_{-0.0008} < 0.0027$	$0.0023^{+0.0014}_{-0.0011} < 0.0039$	$0.0019^{+0.0011}_{-0.0012} < 0.0036$
Ω_{m0}	$0.210^{+0.020+0.12}_{-0.065-0.079}$	$0.265^{+0.012+0.022}_{-0.011-0.022}$	$0.290^{+0.009+0.017}_{-0.009-0.016}$	$0.290^{+0.008+0.016}_{-0.008-0.016}$	$0.263^{+0.011+0.021}_{-0.011-0.020}$	$0.2629^{+0.0078+0.016}_{-0.0078-0.015}$
σ_8	$0.956^{+0.096+0.118}_{-0.039-0.164}$	$0.870^{+0.022+0.044}_{-0.023-0.043}$	$0.831^{+0.017+0.035}_{-0.018-0.034}$	$0.831^{+0.018+0.034}_{-0.018-0.034}$	$0.880^{+0.019+0.040}_{-0.020-0.040}$	$0.873^{+0.018+0.037}_{-0.018-0.036}$
H_0	84^{+12+15}_{-5-19}	$73.5^{+1.6+3.2}_{-1.7-3.2}$	$70.06^{+0.95+2.0}_{-0.98-1.8}$	$70.1^{+1.0+1.9}_{-1.0-1.8}$	$74.0^{+1.5+2.7}_{-1.6-2.8}$	$73.8^{+1.1+2.1}_{-1.1-2.1}$
S_8	$0.807^{+0.045+0.069}_{-0.044-0.074}$	$0.803^{+0.025+0.043}_{-0.021-0.097}$	$0.803^{+0.026+0.043}_{-0.025-0.090}$	$0.800^{+0.028+0.044}_{-0.030-0.090}$	$0.823^{+0.017+0.030}_{-0.016-0.032}$	$0.817^{+0.015+0.030}_{-0.015-0.029}$

summary, as we can see from the results, most of the data sets indicate a nonzero interaction together with the existence of a phantom dark energy. The estimated values of Ω_{m0} are similar to those found in IDE1, especially for its lower value for the CMB-only analysis.

Regarding the estimates of the Hubble parameter H_0, we see that for CMB data alone H_0 acquires a very high value with very large error bars compared to the *Planck* one within the minimal ΛCDM model [116] (in particular, $H_0 = 84^{+14}_{-7}$ at the 68% C.L. for CMB data alone). This is due to the strong correlation between w_0 and H_0. When external data sets (such as BAO, JLA, CC, R19, and their combinations) are added, the estimates of H_0 decrease with a significant reduction in the error bars, but they can still relieve the tension with Ref. [113] within 3 standard deviations.

C. IDE3: Interacting dark energy with $w_x(a) = w_0 a[1 + \sin(1 - a)]$

The summary of the observational constraints for this interaction scenario using different observational data sets is presented in Table IV, and in Figs. 6 and 7 we show the 2D contour plots and 1D posterior distributions for some of the free parameters and data set combinations.

Concerning the coupling parameter, our analysis reveals some interesting features. In particular, as we can see, for CMB data alone we have $\xi = 0$ within 68% C.L. and hence it is consistent with a noninteracting cosmology. Nevertheless, as soon as external data sets (namely, BAO, JLA, CC, or R19) are added in different combinations (such as CMB + BAO, CMB + BAO+ JLA, CMB + BAO + JLA + CC, and CMB + R19) we see that a nonzero interaction is favored at more than 1σ.

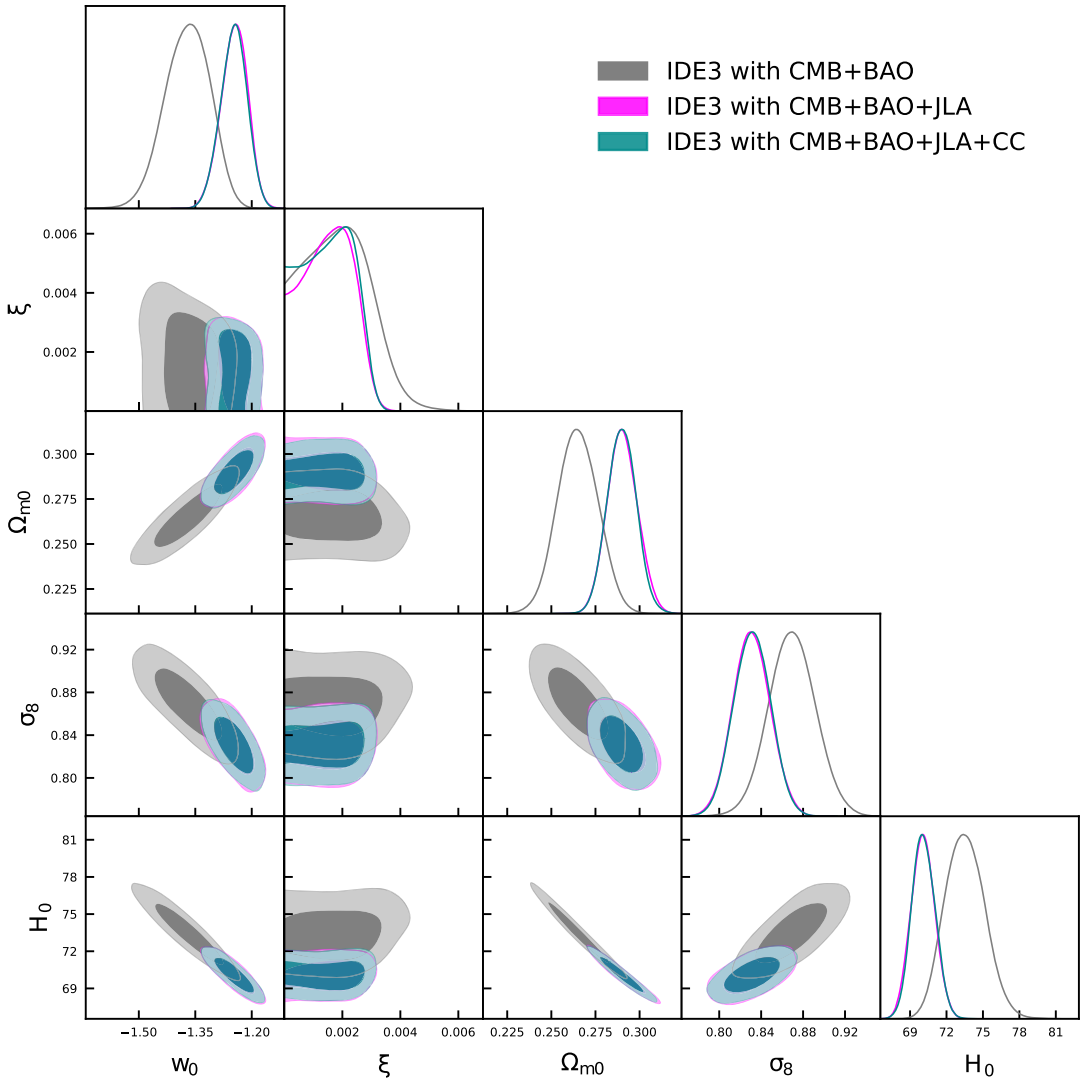

FIG. 6. The 68% and 95% C.L. contour plots between various combinations of the model parameters of scenario IDE3, using different observational astronomical data sets. Additionally, we display the one-dimensional marginalized posterior distributions of some free parameters.

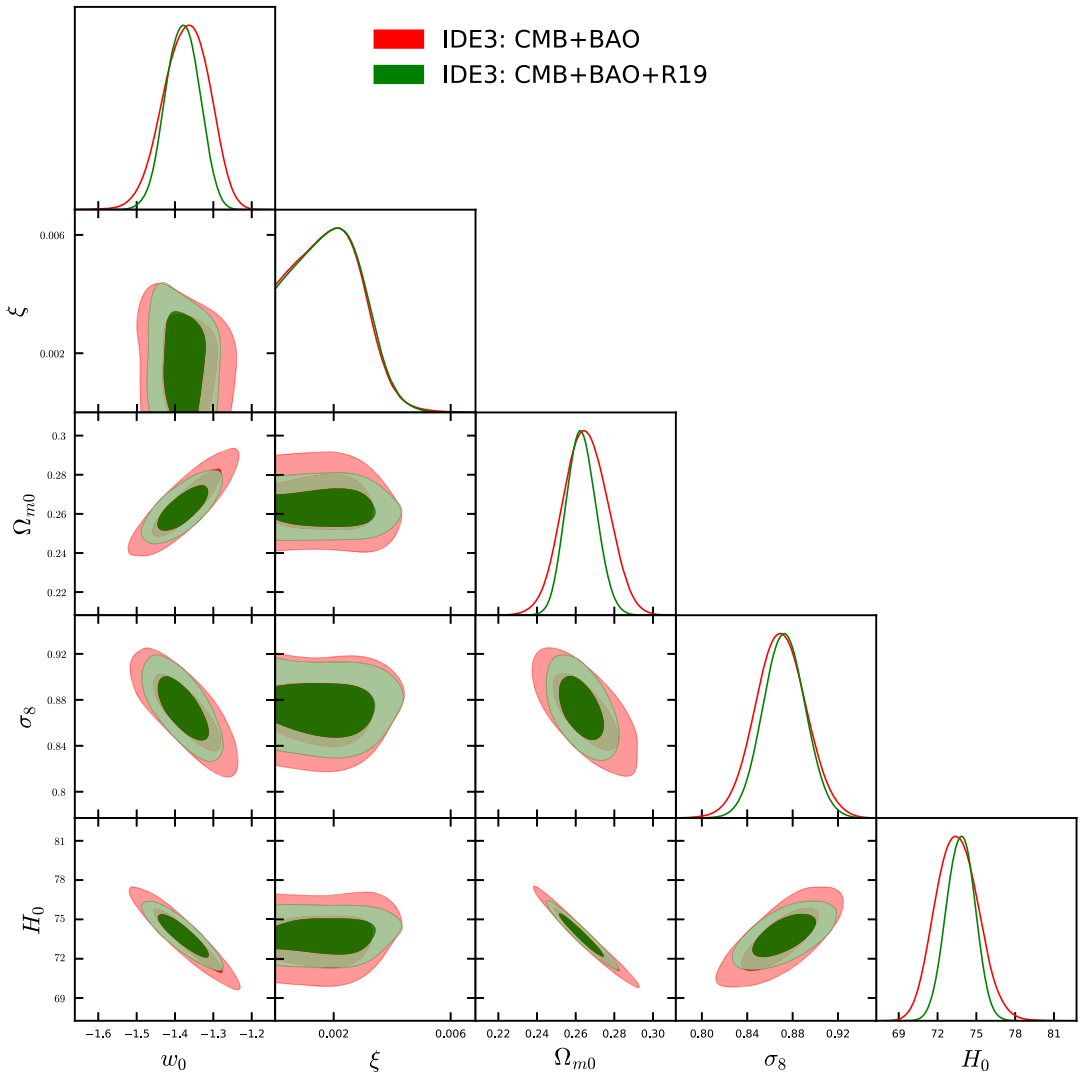

FIG. 7. The 68% and 95% C.L. contour plots between various combinations of the model parameters of scenario IDE3 using only the CMB + BAO and CMB + BAO + R19 data sets, and the corresponding one-dimensional marginalized posterior distributions.

However, we mention that within the 95% C.L. these combinations of observational data sets allow for a non-interacting cosmology. We note that the R19 data has similar effects when combined with CMB and CMB + BAO, as reported previously for IDE2.

Concerning the current value of the dark energy equation of state w_0, we find a similar character to what we already found in IDE1 and IDE2. In particular, the results show that, irrespective of the observational data sets that we have used in this work, w_0 remains less than -1 at more than 95% C.L. (i.e., in the phantom region) for the CMB-only case, and several standard deviations (more than 5) for the combinations with the other cosmological probes. If we compare this table with the results shown in Ref. [83] for the same model without an interaction, we can see that the constraints are very robust, and only the upper limit of w_0 for the CMB-only case is slightly shifted to less phantom values. Furthermore, we mention that in this scenario the CC data set does not improve the constraints at all. Let us note that, similar to IDE1 and IDE2, for the CMB-only analysis Ω_{m0} acquires a lower value compared to *Planck* [117].

Finally, regarding the H_0 parameter we again find a similar behavior to what we observed for IDE1 and IDE2. Since a higher value of the Hubble parameter corresponds to a phantom dark energy equation of state, due to their negative correlation, the highly negative w_0 values that we obtain are accompanied by a high value of H_0 with large asymmetric error bars. Specifically, we find $H_0 = 84^{+12}_{-5}$ at the 68% C.L., which is much higher than the recent ΛCDM-based estimate by *Planck* [116] but in agreement with the direct measurements $H_0 = 73.24 \pm 1.74$ [118], $H_0 = 73.48 \pm 1.66$ [119], or $H_0 = 74.03 \pm 1.42$ [113]. However, after the inclusion of the

TABLE V. 68% and 95% confidence level constraints on the interacting scenario IDE4 with the dark energy equation of state $w_x(a) = w_0 a[1 + \arcsin(1 - a)]$ (Model IV) for various observational data sets. Here Ω_{m0} is the present value of the total matter density parameter $\Omega_m = \Omega_b + \Omega_c$, and H_0 is in units of km/sec/Mpc.

Parameters	CMB	CMB + BAO	CMB + BAO + JLA	CMB + BAO + JLA + CC	CMB + R19	CMB + BAO + R19
$\Omega_c h^2$	$0.1212^{+0.0017+0.0034}_{-0.0019-0.0032}$	$0.1200^{+0.0012+0.0026}_{-0.0012-0.0026}$	$0.1192^{+0.0011+0.0022}_{-0.0011-0.0022}$	$0.1193^{+0.0010+0.0022}_{-0.0011-0.0020}$	$0.1208^{+0.0015+0.0022}_{-0.0013-0.0024}$	$0.1201^{+0.0012+0.0026}_{-0.0012-0.0026}$
$\Omega_b h^2$	$0.02214^{+0.00018+0.00034}_{-0.00018-0.00034}$	$0.02217^{+0.00014+0.00027}_{-0.00015-0.00027}$	$0.02222^{+0.00013+0.00029}_{-0.00014-0.00028}$	$0.02222^{+0.00015+0.00027}_{-0.00014-0.00027}$	$0.02212^{+0.00013+0.00028}_{-0.00017-0.00025}$	$0.02217^{+0.00014+0.00027}_{-0.00015-0.00028}$
$100\theta_{\rm MC}$	$1.04027^{+0.00042+0.00076}_{-0.00034-0.00080}$	$1.04040^{+0.00032+0.00062}_{-0.00032-0.00059}$	$1.04046^{+0.00032+0.00056}_{-0.00026-0.00057}$	$1.04050^{+0.00031+0.00059}_{-0.00030-0.00060}$	$1.04027^{+0.00036+0.00057}_{-0.00031-0.00060}$	$1.04040^{+0.00033+0.00060}_{-0.00031-0.00058}$
τ	$0.079^{+0.019+0.032}_{-0.017-0.034}$	$0.089^{+0.018+0.033}_{-0.017-0.034}$	$0.096^{+0.016+0.034}_{-0.016-0.034}$	$0.096^{+0.019+0.036}_{-0.016-0.036}$	$0.077^{+0.025+0.035}_{-0.018-0.038}$	$0.088^{+0.018+0.033}_{-0.017-0.033}$
n_s	$0.9721^{+0.0044+0.0092}_{-0.0047-0.0087}$	$0.9741^{+0.0042+0.0081}_{-0.0042-0.0082}$	$0.9765^{+0.0040+0.0082}_{-0.0044-0.0080}$	$0.9764^{+0.0038+0.0075}_{-0.0038-0.0078}$	$0.9721^{+0.0046+0.0078}_{-0.0036-0.0084}$	$0.9739^{+0.0042+0.0081}_{-0.0042-0.0080}$
$\ln(10^{10}A_s)$	$3.103^{+0.037+0.063}_{-0.031-0.067}$	$3.120^{+0.035+0.066}_{-0.033-0.067}$	$3.132^{+0.034+0.064}_{-0.032-0.064}$	$3.132^{+0.037+0.069}_{-0.032-0.071}$	$3.099^{+0.048+0.067}_{-0.034-0.076}$	$3.118^{+0.035+0.064}_{-0.032-0.066}$
w_0	$< -1.48 < -1.02$	$-1.331^{+0.067+0.12}_{-0.056-0.13}$	$-1.218^{+0.040+0.067}_{-0.029-0.074}$	$-1.222^{+0.038+0.065}_{-0.033-0.072}$	$-1.394^{+0.045+0.098}_{-0.048-0.092}$	$-1.353^{+0.048+0.084}_{-0.043-0.091}$
ξ	$<0.0041 < 0.0093$	$<0.0028 < 0.0042$	$0.0017^{+0.0011}_{-0.0011} < 0.0032$	$0.0018^{+0.0012}_{-0.0011} < 0.0033$	$<0.0030 < 0.0044$	$<0.0030 < 0.0042$
Ω_{m0}	$0.229^{+0.098+0.15}_{-0.089-0.096}$	$0.270^{+0.011+0.023}_{-0.012-0.022}$	$0.2919^{+0.0078+0.016}_{-0.0080-0.016}$	$0.291^{+0.0079+0.016}_{-0.0080-0.016}$	$0.260^{+0.011+0.024}_{-0.011-0.023}$	$0.2648^{+0.0078+0.016}_{-0.0080-0.015}$
σ_8	$0.93^{+0.12+0.14}_{-0.14-0.18}$	$0.867^{+0.023+0.046}_{-0.023-0.045}$	$0.832^{+0.016+0.034}_{-0.018-0.032}$	$0.834^{+0.017+0.034}_{-0.017-0.033}$	$0.881^{+0.024+0.039}_{-0.020-0.043}$	$0.874^{+0.019+0.038}_{-0.019-0.037}$
H_0	82^{+14+16}_{-17-21}	$72.8^{+1.5+3.3}_{-1.8-3.0}$	$69.8^{+0.8+1.9}_{-1.0-1.8}$	$69.9^{+0.9+2.0}_{-1.0-1.8}$	$74.3^{+1.5+3.1}_{-1.4-3.2}$	$73.5^{+1.1+2.2}_{-1.2-2.1}$
S_8	$0.818^{+0.041+0.065}_{-0.045-0.074}$	$0.812^{+0.022+0.039}_{-0.019-0.066}$	$0.808^{+0.022+0.040}_{-0.022-0.073}$	$0.810^{+0.022+0.038}_{-0.021-0.070}$	$0.820^{+0.017+0.036}_{-0.018-0.040}$	$0.821^{+0.016+0.032}_{-0.016-0.033}$

external data sets such as BAO, JLA, CC, and R19, we find that H_0 decreases with respect to its estimate from CMB data alone, and additionally its error bars are significantly reduced.

In summary, we find that the alleviation of the H_0 tension is more robust in this scenario compared to IDE1 and IDE2 (see also Fig 3). Indeed, the estimated values of H_0 from the different combinations of observational data sets are as follows:

(1) CMB + BAO: $H_0 = 73.5^{+1.6}_{-1.7}$ at the 68% C.L. ($H_0 = 73.5 \pm 3.2$ at the 95% C.L.);
(2) CMB + BAO + JLA: $H_0 = 70.06^{+0.95}_{-0.98}$ at the 68% C.L. ($H_0 = 70.1^{+2.0}_{-1.8}$ at the 95% C.L.);
(3) CMB + BAO + JLA + CC: $H_0 = 70.1 \pm 1.0$ at the 68% C.L. ($H_0 = 70.1^{+1.9}_{-1.8}$ at the 95% C.L.),

where the first one is in perfect agreement with Ref. [113], and the last two alleviate the tension at about 2σ.

D. IDE4: Interacting dark energy with $w_x(a) = w_0 a[1 + \arcsin(1-a)]$

The summary of the observational constraints for this interacting scenario using different observational data sets is displayed in Table V, and in Figs. 8 and 9 we present the 2D contour plots and 1D posterior distributions. The behavior of this interaction scenario has some similarities to that of IDE1. Looking at the results, in this case we also find that for the analysis with the CMB-only and CMB + BAO data sets, the coupling parameter is consistent with $\xi = 0$ within the 68% C.L. The addition of JLA or CC data (namely, the data-set combinations CMB + BAO + JLA and CMB + BAO+ JLA + CC) instead gives an indication that $\xi \neq 0$ at more than 68% C.L., but it is always in agreement with zero within 2σ. We mention that, similar to the previous IDE1 scenarios, here we also see that the addition of R19 data to CMB and CMB + BAO data improves the constraints on ξ; however, it only gives an upper bound on it.

Concerning the dark energy equation-of-state parameter at present, we extract a similar conclusion to the previous interacting scenario IDE3, namely, we find that $w_0 < -1$ at more than 95% C.L. for the CMB-only case, and several standard deviations for its combination with the external data sets. Furthermore, for this scenario the CMB-only case has a slightly less phantom w_0 than the same case without an interaction, as can be seen in Ref. [83]. As already reported in earlier IDE models, Ω_{m0} for the CMB-only case obtains a lower value, contrary to *Planck* observations [117].

Now we focus on the trend of the Hubble parameter H_0. For the data sets we use, in this case it is again anticorrelated with w_0, as we can see in Fig. 8. We note that, similar to the previous interaction scenarios, the CMB-only fit gives a very high value for H_0 with large error bars, which are reduced after the inclusion of the external data

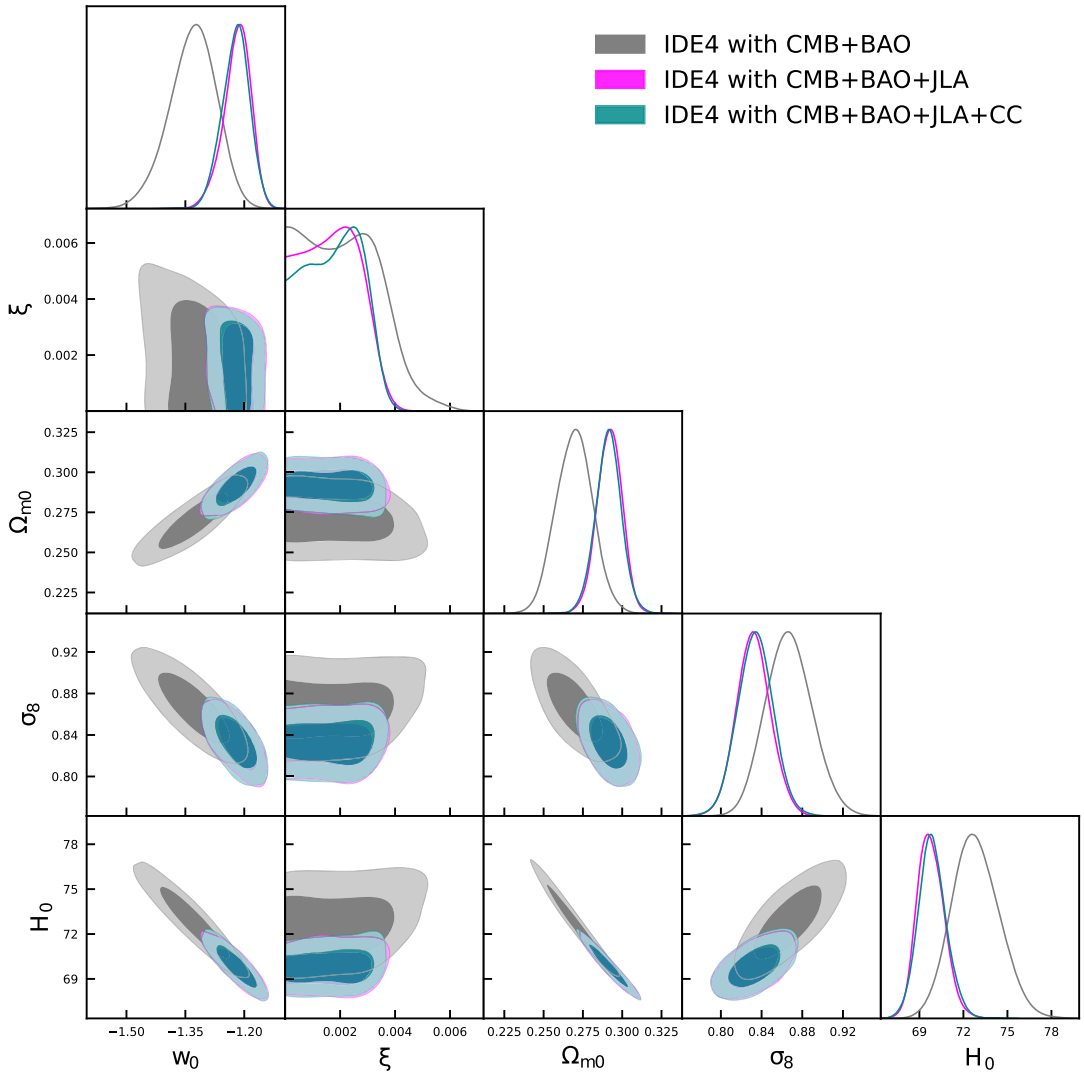

FIG. 8. The 68% and 95% C.L. contour plots between various combinations of the model parameters of scenario IDE4, using different observational astronomical data sets. Additionally, we display the one-dimensional marginalized posterior distributions of some free parameters.

sets such as BAO, JLA, and CC. For this scenario we also conclude that the tension with the direct measurements [113,118,119] is solved for the CMB and CMB + BAO cases, while with the addition of JLA and JLA + CC it is at about 2σ. For this reason, we can safely add the R19 measurements to the CMB and CMB + BAO data, and we show the results in the last two columns of Table V.

V. BAYESIAN EVIDENCE

In this section we compute the Bayesian evidences of all of the examined interacting models in order to compare their observational soundness with respect to some reference model, and in particular to ΛCDM cosmology. We use the publicly available code MCEvidence [120,121] to compute the evidences, since the code directly accepts the Markov chain Monte Carlo chains of the analysis. We refer to Ref. [83] for discussions on Bayesian evidence analysis, and in Table VI we provide the revised Jeffreys scale by Kass and Raftery [122].

For all of the examined scenarios we compute the values of $\ln B_{ij}$, which are summarized in Table VII. From this table one can see that the ΛCDM paradigm is usually preferred over the present IDE models, with the exception of the CMB + R19 combination, where we see a weak/positive evidence for all IDE models against ΛCDM. This is expected since the number of free parameters of all IDE models is eight, that is, two more than the six parameters of ΛCDM.

VI. CONCLUDING REMARKS

Interacting scenarios have attracted much interest as they are efficient at alleviating the coincidence problem, and

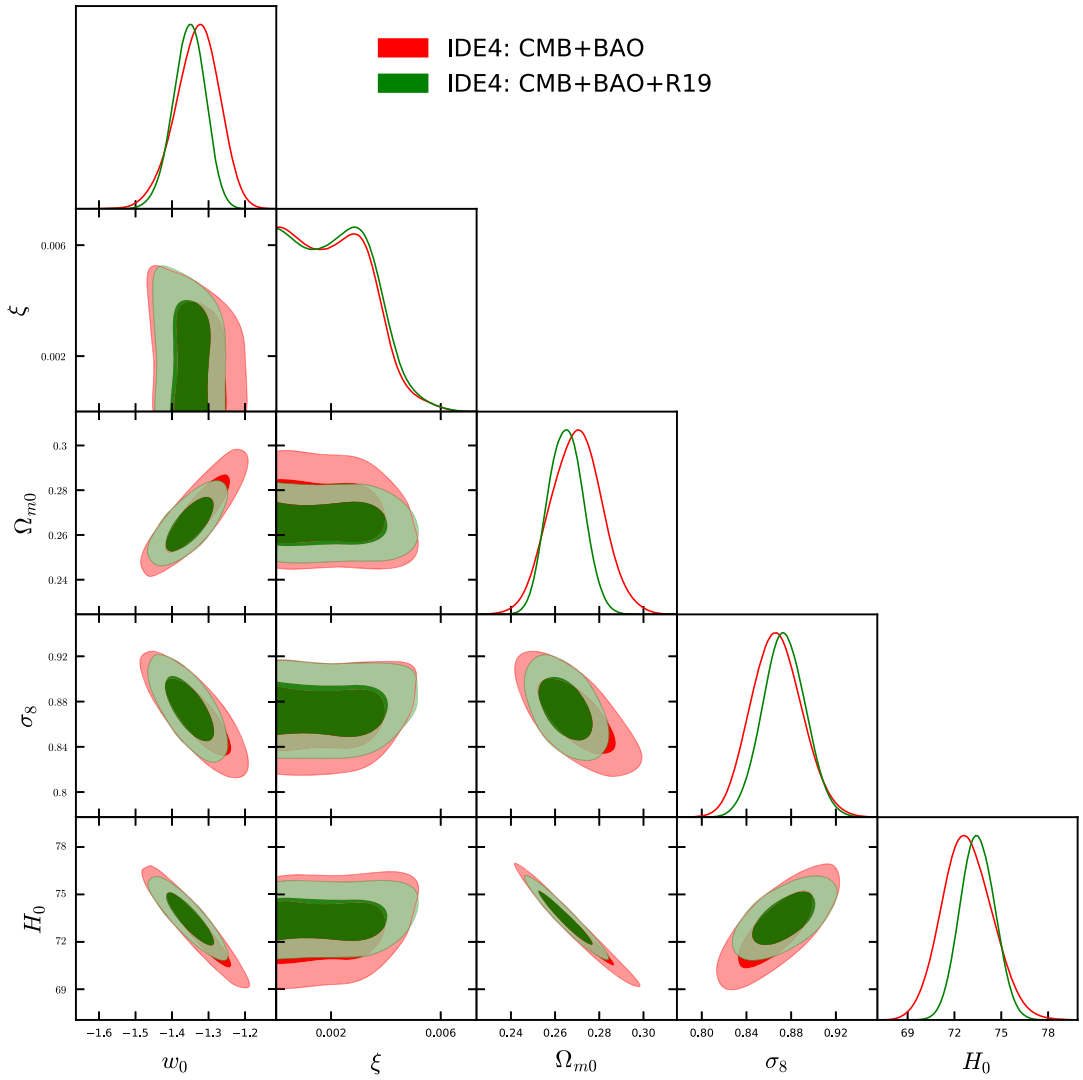

FIG. 9. The 68% and 95% C.L. contour plots between various combinations of the model parameters of scenario IDE4 using only the CMB + BAO and CMB + BAO + R19 data sets, and the corresponding one-dimensional marginalized posterior distributions.

additionally they seem to alleviate the H_0 tension and σ_8 tensions. In the present work we investigated interacting scenarios that belong to a wider class, since they include a dynamical dark energy component whose equation of state follows various one-parameter parametrizations. In particular, our focus was to see if a nonzero interaction is favored, and if the H_0 tension is still alleviated.

TABLE VI. Revised Jeffreys scale [122] that quantifies the comparison of the models.

$\ln B_{ij}$	Strength of evidence for model M_i
$0 \leq \ln B_{ij} < 1$	Weak
$1 \leq \ln B_{ij} < 3$	Definite/Positive
$3 \leq \ln B_{ij} < 5$	Strong
$\ln B_{ij} \geq 5$	Very strong

We considered a well-known interaction of the form $Q = 3H\xi(1+w_x)\rho_x$, and we took the dark energy equation-of-state parameter w_x to be $w_x(a) = w_0 a[1 - \log(a)]$ (Model IDE1), $w_x = w_0 a \exp(1-a)$ (Model IDE2), $w_x(a) = w_0 a[1 + \sin(1-a)]$ (Model IDE3), or $w_x(a) = w_0 a[1 + \arcsin(1-a)]$ (Model IDE4). Additionally, we used the latest observational data from CMB, JLA, BAO, Hubble parameter measurements from CCs, and a Gaussian prior on H_0 labeled as R19 from SH0ES [113].

Our analysis shows that the coupling strength for all interacting scenarios is quite small, and thus the models are consistent with the noninteracting w_x cosmology. In particular, all scenarios are in agreement with $\xi = 0$ within 2σ, but an indication for ξ greater than zero appears at 1σ when JLA and JLA + CC are added to CMB + BAO, or when R19 is added to both CMB and CMB + BAO in the IDE1 and IDE2 scenarios.

TABLE VII. The values of $\ln B_{ij}$, where j stands for the reference model ΛCDM and i stands for the IDE models. A negative sign indicates that the reference model is favored over the IDE models.

Data set	Model	$\ln B_{ij}$	Strength of evidence for reference model ΛCDM
CMB	IDE1	−2.8	Definite/Positive
CMB + BAO	IDE1	−4.6	Strong
CMB + BAO + JLA	IDE1	−7.3	Very strong
CMB + BAO + JLA + CC	IDE1	−6.7	Very strong
CMB + R19	IDE1	+1.0	Weak for IDE1
CMB + BAO + R19	IDE1	−0.7	Weak
CMB	IDE2	−4.3	Strong
CMB + BAO	IDE2	−4.9	Strong
CMB + BAO + JLA	IDE2	−8.3	Very strong
CMB + BAO + JLA + CC	IDE2	−8.9	Very strong
CMB + R19	IDE2	+1.6	Definite/Positive for IDE2
CMB + BAO + R19	IDE2	−2.2	Definite/Positive
CMB	IDE3	−2.1	Definite/Positive
CMB + BAO	IDE3	−7.6	Strong
CMB + BAO + JLA	IDE3	−8.8	Strong
CMB + BAO + JLA + CC	IDE3	−9.5	Strong
CMB + R19	IDE3	+2.0	Definite/Positive for IDE3
CMB + BAO + R19	IDE3	−1.1	Definite/Positive
CMB	IDE4	−2.0	Definite/Positive
CMB + BAO	IDE4	−5.2	Definite/Positive
CMB + BAO + JLA	IDE4	−9.6	Strong
CMB + BAO + JLA + CC	IDE4	−9.7	Strong
CMB + R19	IDE4	+0.9	Weak for IDE4
CMB + BAO + R19	IDE4	−2.3	Definite/Positive

Concerning the current value of the dark energy equation of state w_0, for all interacting scenarios and for all combinations of data sets it always lies in the phantom regime at more than 2–3 standard deviations. Moreover, we find a robust anticorrelation between w_0 and H_0.

However, the most striking feature, and one of the main results of the present work, is that for all interacting models—independent of the combination of data sets considered—the estimated values of the Hubble parameter H_0 are greater compared to the ΛCDM-based *Planck* estimate [117] and close to the local measurements of H_0 from Refs. [113,118,119]. This is triggered by the aforementioned anticorrelation between w_0 and H_0 and the strongly phantom values we obtained for w_0. The alleviation of H_0 tension is independent of the interaction model due to the absence of correlation between ξ and H_0, as shown in the two-dimensional joint contours obtained for all observational data sets.

In summary, the extended interacting scenarios that include dark energy sectors with a dynamical equation of state with only one free parameter are very efficient at alleviating the H_0 tension.

ACKNOWLEDGMENTS

The authors thank the referee for some important comments that improved the discussion of the article. S. P. has been supported by the Mathematical Research Impact-Centric Support Scheme (MATRICS), File No. MTR/2018/000940, given by the Science and Engineering Research Board (SERB), Govt. of India, as well as by the Faculty Research and Professional Development Fund (FRPDF) Scheme of Presidency University, Kolkata, India. W. Y. was supported by the National Natural Science Foundation of China under Grants No. 11705079 and No. 11647153. E. D. V. was supported by the European Research Council in the form of a Consolidator Grant No. 681431. S. C. acknowledges MATRICS, File No. MTR/2017/000407. This article is based on work from CANTATA COST (European Cooperation in Science and Technology) action CA15117, EU Framework Programme Horizon 2020.

[1] E. J. Copeland, M. Sami, and S. Tsujikawa, Dynamics of dark energy, Int. J. Mod. Phys. D **15**, 1753 (2006).

[2] S. Capozziello and M. De Laurentis, Extended theories of gravity, Phys. Rep. **509**, 167 (2011).

[3] Y. F. Cai, S. Capozziello, M. De Laurentis, and E. N. Saridakis, f(T) teleparallel gravity and cosmology, Rep. Prog. Phys. **79**, 106901 (2016).

[4] S. Nojiri, S. D. Odintsov, and V. K. Oikonomou, Modified gravity theories on a Nutshell: Inflation, bounce and late-time evolution, Phys. Rep. **692**, 1 (2017).

[5] C. Wetterich, The cosmon model for an asymptotically vanishing time-dependent cosmological constant, Astron. Astrophys. **301**, 321 (1995).

[6] L. Amendola, Coupled quintessence, Phys. Rev. D **62**, 043511 (2000).

[7] L. Amendola and C. Quercellini, Tracking and coupled dark energy as seen by WMAP, Phys. Rev. D **68**, 023514 (2003).

[8] R. G. Cai and A. Wang, Cosmology with interaction between phantom dark energy and dark matter and the coincidence problem, J. Cosmol. Astropart. Phys. 03 (2005) 002.

[9] D. Pavón and W. Zimdahl, Holographic dark energy and cosmic coincidence, Phys. Lett. B **628**, 206 (2005).

[10] S. del Campo, R. Herrera, and D. Pavón, Toward a solution of the coincidence problem, Phys. Rev. D **78**, 021302 (2008).

[11] S. del Campo, R. Herrera, and D. Pavón, Interacting models may be key to solve the cosmic coincidence problem, J. Cosmol. Astropart. Phys. 01 (2009) 020.

[12] J. D. Barrow and T. Clifton, Cosmologies with energy exchange, Phys. Rev. D **73**, 103520 (2006).

[13] L. Amendola, G. Camargo Campos, and R. Rosenfeld, Consequences of dark matter-dark energy interaction on cosmological parameters derived from SNIa data, Phys. Rev. D **75**, 083506 (2007).

[14] J. H. He and B. Wang, Effects of the interaction between dark energy and dark matter on cosmological parameters, J. Cosmol. Astropart. Phys. 06 (2008) 010.

[15] X. m. Chen, Y. g. Gong, and E. N. Saridakis, Phase-space analysis of interacting phantom cosmology, J. Cosmol. Astropart. Phys. 04 (2009) 001.

[16] S. Basilakos and M. Plionis, Is the interacting dark matter scenario an alternative to dark energy?, Astron. Astrophys. **507**, 47 (2009).

[17] M. B. Gavela, D. Hernandez, L. Lopez Honorez, O. Mena, and S. Rigolin, Dark coupling, J. Cosmol. Astropart. Phys. 07 (2009) 034.

[18] H. M. Sadjadi, $w(d) = -1$ in interacting quintessence model, Eur. Phys. J. C **66**, 445 (2010).

[19] M. Jamil, E. N. Saridakis, and M. R. Setare, Thermodynamics of dark energy interacting with dark matter and radiation, Phys. Rev. D **81**, 023007 (2010).

[20] X. m. Chen, Y. Gong, E. N. Saridakis, and Y. Gong, Time-dependent interacting dark energy and transient acceleration, Int. J. Theor. Phys. **53**, 469 (2014).

[21] S. Pan and S. Chakraborty, Will there be again a transition from acceleration to deceleration in course of the dark energy evolution of the universe?, Eur. Phys. J. C **73**, 2575 (2013).

[22] W. Yang and L. Xu, Testing coupled dark energy with large scale structure observation, J. Cosmol. Astropart. Phys. 08 (2014) 034.

[23] W. Yang and L. Xu, Cosmological constraints on interacting dark energy with redshift-space distortion after Planck data, Phys. Rev. D **89**, 083517 (2014).

[24] R. C. Nunes and E. M. Barboza, Dark matter-dark energy interaction for a time-dependent EoS parameter, Gen. Relativ. Gravit. **46**, 1820 (2014).

[25] V. Faraoni, J. B. Dent, and E. N. Saridakis, Covariantizing the interaction between dark energy and dark matter, Phys. Rev. D **90**, 063510 (2014).

[26] V. Salvatelli, N. Said, M. Bruni, A. Melchiorri, and D. Wands, Indications of a Late-Time Interaction in the Dark Sector, Phys. Rev. Lett. **113**, 181301 (2014).

[27] W. Yang and L. Xu, Coupled dark energy with perturbed Hubble expansion rate, Phys. Rev. D **90**, 083532 (2014).

[28] S. Pan, S. Bhattacharya, and S. Chakraborty, An analytic model for interacting dark energy and its observational constraints, Mon. Not. R. Astron. Soc. **452**, 3038 (2015).

[29] Y. H. Li, J. F. Zhang, and X. Zhang, Testing models of vacuum energy interacting with cold dark matter, Phys. Rev. D **93**, 023002 (2016).

[30] R. C. Nunes, S. Pan, and E. N. Saridakis, New constraints on interacting dark energy from cosmic chronometers, Phys. Rev. D **94**, 023508 (2016).

[31] W. Yang, H. Li, Y. Wu, and J. Lu, Cosmological constraints on coupled dark energy, J. Cosmol. Astropart. Phys. 10 (2016) 007.

[32] S. Kumar and R. C. Nunes, Probing the interaction between dark matter and dark energy in the presence of massive neutrinos, Phys. Rev. D **94**, 123511 (2016).

[33] S. Pan and G. S. Sharov, A model with interaction of dark components and recent observational data, Mon. Not. R. Astron. Soc. **472**, 4736 (2017).

[34] A. Mukherjee and N. Banerjee, In search of the dark matter dark energy interaction: A kinematic approach, Classical Quantum Gravity **34**, 035016 (2017).

[35] R. Erdem, Is it possible to obtain cosmic accelerated expansion through energy transfer between different energy densities?, Phys. Dark Universe **15**, 57 (2017).

[36] G. S. Sharov, S. Bhattacharya, S. Pan, R. C. Nunes, and S. Chakraborty, A new interacting two fluid model and its consequences, Mon. Not. R. Astron. Soc. **466**, 3497 (2017).

[37] M. Shahalam, S. D. Pathak, S. Li, R. Myrzakulov, and A. Wang, Dynamics of coupled phantom and tachyon fields, Eur. Phys. J. C **77**, 686 (2017).

[38] R. Y. Guo, Y. H. Li, J. F. Zhang, and X. Zhang, Weighing neutrinos in the scenario of vacuum energy interacting with cold dark matter: Application of the parameterized post-Friedmann approach, J. Cosmol. Astropart. Phys. 05 (2017) 040.

[39] R. G. Cai, N. Tamanini, and T. Yang, Reconstructing the dark sector interaction with LISA, J. Cosmol. Astropart. Phys. 05 (2017) 031.

[40] W. Yang, N. Banerjee, and S. Pan, Constraining a dark matter and dark energy interaction scenario with a dynamical equation of state, Phys. Rev. D **95**, 123527 (2017).

[41] L. Santos, W. Zhao, E. G. M. Ferreira, and J. Quintin, Constraining interacting dark energy with CMB and BAO future surveys, Phys. Rev. D **96**, 103529 (2017).
[42] W. Yang, S. Pan, and D. F. Mota, Novel approach toward the large-scale stable interacting dark-energy models and their astronomical bounds, Phys. Rev. D **96**, 123508 (2017).
[43] C. Van De Bruck and J. Mifsud, Searching for dark matter—dark energy interactions: Going beyond the conformal case, Phys. Rev. D **97**, 023506 (2018).
[44] S. Pan, A. Mukherjee, and N. Banerjee, Astronomical bounds on a cosmological model allowing a general interaction in the dark sector, Mon. Not. R. Astron. Soc. **477**, 1189 (2018).
[45] X. Xu, Y. Z. Ma, and A. Weltman, Constraining the interaction between dark sectors with future HI intensity mapping observations, Phys. Rev. D **97**, 083504 (2018).
[46] W. Yang, S. Pan, R. Herrera, and S. Chakraborty, Large-scale (in) stability analysis of an exactly solved coupled dark-energy model, Phys. Rev. D **98**, 043517 (2018).
[47] W. Yang, S. Pan, L. Xu, and D. F. Mota, Effects of anisotropic stress in interacting dark matter-dark energy scenarios, Mon. Not. R. Astron. Soc. **482**, 1858 (2019).
[48] W. Yang, S. Pan, and A. Paliathanasis, Cosmological constraints on an exponential interaction in the dark sector, Mon. Not. R. Astron. Soc. **482**, 1007 (2019).
[49] D. Grandon and V. H. Cardenas, Exploring evidence of interaction between dark energy and dark matter, Gen. Relativ. Gravit. **51**, 42 (2019).
[50] S. D. Odintsov and V. K. Oikonomou, Study of finite-time singularities of loop quantum cosmology interacting multi-fluids, Phys. Rev. D **97**, 124042 (2018).
[51] R. von Marttens, L. Casarini, D. F. Mota, and W. Zimdahl, Cosmological constraints on parametrized interacting dark energy, Phys. Dark Universe **23**, 100248 (2019).
[52] W. Yang, N. Banerjee, A. Paliathanasis, and S. Pan, Reconstructing the dark matter and dark energy interaction scenarios from observations, Phys. Dark Universe **26**, 100383 (2019).
[53] M. Bonici and N. Maggiore, Constraints on interacting dynamical dark energy from the cosmological equation of state, Eur. Phys. J. C **79**, 672 (2019).
[54] M. Asghari, J. B. Jiménez, S. Khosravi, and D. F. Mota, On structure formation from a small-scales-interacting dark sector, J. Cosmol. Astropart. Phys. 04 (2019) 042.
[55] A. Paliathanasis, S. Pan, and W. Yang, Dynamics of nonlinear interacting dark energy models, Int. J. Mod. Phys. D **28**, 1950161 (2019).
[56] S. Pan, W. Yang, C. Singha, and E. N. Saridakis, Observational constraints on sign-changeable interaction models and alleviation of the H_0 tension, Phys. Rev. D **100**, 083539 (2019).
[57] L. Feng, H. L. Li, J. F. Zhang, and X. Zhang, Exploring neutrino mass and mass hierarchy in interacting dark energy models, Sci. China Phys. Mech. Astron. **63**, 220401 (2020).
[58] C. Li, X. Ren, M. Khurshudyan, and Y. F. Cai, Implications of the possible 21-cm line excess at cosmic dawn on dynamics of interacting dark energy, arXiv:1904.02458.
[59] W. Yang, S. Pan, E. Di Valentino, B. Wang, and A. Wang, Forecasting interacting vacuum-energy models using gravitational waves, arXiv:1904.11980.
[60] W. Yang, S. Vagnozzi, E. Di Valentino, R. C. Nunes, S. Pan, and D. F. Mota, Listening to the sound of dark sector interactions with gravitational wave standard sirens, J. Cosmol. Astropart. Phys. 07 (2019) 037.
[61] V. K. Oikonomou, Generalized logarithmic equation of state in classical and loop quantum cosmology dark energy-dark matter coupled systems, Ann. Phys. (Amsterdam) **409**, 167934 (2019).
[62] Y. L. Bolotin, A. Kostenko, O. A. Lemets, and D. A. Yerokhin, Cosmological evolution with interaction between dark energy and dark matter, Int. J. Mod. Phys. D **24**, 1530007 (2015).
[63] B. Wang, E. Abdalla, F. Atrio-Barandela, and D. Pavón, Dark matter and dark energy interactions: Theoretical challenges, cosmological implications and observational signatures, Rep. Prog. Phys. **79**, 096901 (2016).
[64] B. Wang, Y. g. Gong, and E. Abdalla, Transition of the dark energy equation of state in an interacting holographic dark energy model, Phys. Lett. B **624**, 141 (2005).
[65] H. M. Sadjadi and M. Honardoost, Thermodynamics second law and $omega = -1$ crossing(s) in interacting holographic dark energy model, Phys. Lett. B **647**, 231 (2007).
[66] S. Pan and S. Chakraborty, A cosmographic analysis of holographic dark energy models, Int. J. Mod. Phys. D **23**, 1450092 (2014).
[67] E. Di Valentino, A. Melchiorri, and J. Silk, Beyond six parameters: Extending ΛCDM, Phys. Rev. D **92**, 121302 (2015).
[68] E. Di Valentino, A. Melchiorri, and J. Silk, Reconciling Planck with the local value of H_0 in extended parameter space, Phys. Lett. B **761**, 242 (2016).
[69] S. Kumar and R. C. Nunes, Echo of interactions in the dark sector, Phys. Rev. D **96**, 103511 (2017).
[70] E. Di Valentino, A. Melchiorri, and O. Mena, Can interacting dark energy solve the H_0 tension?, Phys. Rev. D **96**, 043503 (2017).
[71] E. Di Valentino, A. Melchiorri, E. V. Linder, and J. Silk, Constraining dark energy dynamics in extended parameter space, Phys. Rev. D **96**, 023523 (2017).
[72] J. Renk, M. Zumalacárregui, F. Montanari, and A. Barreira, Galileon gravity in light of ISW, CMB, BAO and H_0 data, J. Cosmol. Astropart. Phys. 10 (2017) 020.
[73] E. Di Valentino, Crack in the cosmological paradigm, Nat. Astron. **1**, 569 (2017).
[74] E. Di Valentino, C. Bøehm, E. Hivon, and F. R. Bouchet, Reducing the H_0 and σ_8 tensions with dark matter-neutrino interactions, Phys. Rev. D **97**, 043513 (2018).
[75] D. F. Arenas, E. Terlevich, R. Terlevich, J. Melnick, R. Chávez, F. Bresolin, E. Telles, M. Plionis, and S. Basilakos, An independent determination of the local Hubble constant, Mon. Not. R. Astron. Soc. **474**, 1250 (2018).
[76] E. Di Valentino, E. V. Linder, and A. Melchiorri, Vacuum phase transition solves the H_0 tension, Phys. Rev. D **97**, 043528 (2018).
[77] N. Khosravi, S. Baghram, N. Afshordi, and N. Altamirano, H_0 tension as a hint for a transition in gravitational theory, Phys. Rev. D **99**, 103526 (2019).
[78] E. Mörtsell and S. Dhawan, Does the Hubble constant tension call for new physics?, J. Cosmol. Astropart. Phys. 09 (2018) 025.

[79] W. Yang, S. Pan, E. Di Valentino, R. C. Nunes, S. Vagnozzi, and D. F. Mota, Tale of stable interacting dark energy, observational signatures, and the H_0 tension, J. Cosmol. Astropart. Phys. 09 (2018) 019.
[80] F. D'Eramo, R. Z. Ferreira, A. Notari, and J. L. Bernal, Hot axions and the H_0 tension, J. Cosmol. Astropart. Phys. 11 (2018) 014.
[81] W. Yang, A. Mukherjee, E. Di Valentino, and S. Pan, Interacting dark energy with time varying equation of state and the H_0 tension, Phys. Rev. D **98**, 123527 (2018).
[82] R. Y. Guo, J. F. Zhang, and X. Zhang, Can the H_0 tension be resolved in extensions to ΛCDM cosmology? J. Cosmol. Astropart. Phys. 02 (2019) 054.
[83] W. Yang, S. Pan, E. Di Valentino, E. N. Saridakis, and S. Chakraborty, Observational constraints on one-parameter dynamical dark-energy parametrizations and the H_0 tension, Phys. Rev. D **99**, 043543 (2019).
[84] V. Poulin, T. L. Smith, T. Karwal, and M. Kamionkowski, Early Dark Energy Can Resolve The Hubble Tension, Phys. Rev. Lett. **122**, 221301 (2019).
[85] X. Zhang and Q. G. Huang, Constraints on H_0 from WMAP and baryon acoustic osillation measurements, Commun. Theor. Phys. **71**, 826 (2019).
[86] C. D. Kreisch, F. Y. Cyr-Racine, and O. Doré, The neutrino puzzle: Anomalies, interactions, and cosmological tensions, arXiv:1902.00534.
[87] M. Martinelli, N. B. Hogg, S. Peirone, M. Bruni, and D. Wands, Constraints on the interacting vacuum—geodesic CDM scenario, Mon. Not. R. Astron. Soc. **488**, 3423 (2019).
[88] K. L. Pandey, T. Karwal, and S. Das, Alleviating the H_0 and σ_8 anomalies with a decaying dark matter model, arXiv:1902.10636.
[89] K. Vattis, S. M. Koushiappas, and A. Loeb, Dark matter decaying in the late Universe can relieve the H0 tension, Phys. Rev. D **99**, 121302 (2019).
[90] S. Kumar, R. C. Nunes, and S. K. Yadav, Dark sector interaction: A remedy of the tensions between CMB and LSS data, Eur. Phys. J. C **79**, 576 (2019).
[91] P. Agrawal, F. Y. Cyr-Racine, D. Pinner, and L. Randall, Rock 'n' Roll solutions to the Hubble tension, arXiv:1904.01016.
[92] W. Yang, S. Pan, E. Di Valentino, A. Paliathanasis, and J. Lu, Challenging bulk viscous unified scenarios with cosmological observations, arXiv:1906.04162 [Phys. Rev. D (to be published)].
[93] W. Yang, O. Mena, S. Pan, and E. Di Valentino, Dark sectors with dynamical coupling, Phys. Rev. D **100**, 083509 (2019).
[94] E. Di Valentino, R. Z. Ferreira, L. Visinelli, and U. Danielsson, Late time transitions in the quintessence field and the H_0 tension, Phys. Dark Universe **26**, 100385 (2019).
[95] W. Yang, S. Pan, S. Vagnozzi, E. Di Valentino, D. F. Mota, and S. Capozziello, Dawn of the dark: Unified dark sectors and the EDGES cosmic dawn 21-cm signal, arXiv:1907.05344.
[96] A. Pourtsidou and T. Tram, Reconciling CMB and structure growth measurements with dark energy interactions, Phys. Rev. D **94**, 043518 (2016).
[97] R. An, C. Feng, and B. Wang, Relieving the tension between weak lensing and cosmic microwave background with interacting dark matter and dark energy models, J. Cosmol. Astropart. Phys. 02 (2018) 038.
[98] E. Di Valentino and S. Bridle, Exploring the tension between current cosmic microwave background and cosmic shear data, Symmetry **10**, 585 (2018).
[99] W. Yang, S. Pan, and J. D. Barrow, Large-scale stability and astronomical constraints for coupled dark-energy models, Phys. Rev. D **97**, 043529 (2018).
[100] V. F. Mukhanov, H. A. Feldman, and R. H. Brandenberger, Theory of cosmological perturbations, Phys. Rep. **215**, 203 (1992).
[101] C. P. Ma and E. Bertschinger, Cosmological perturbation theory in the synchronous and conformal Newtonian gauges, Astrophys. J. **455**, 7 (1995).
[102] K. A. Malik and D. Wands, Cosmological perturbations, Phys. Rep. **475**, 1 (2009).
[103] E. Majerotto, J. Valiviita, and R. Maartens, Adiabatic initial conditions for perturbations in interacting dark energy models, Mon. Not. R. Astron. Soc. **402**, 2344 (2010).
[104] J. Väliviita, E. Majerotto, and R. Maartens, Instability in interacting dark energy and dark matter fluids, J. Cosmol. Astropart. Phys. 07 (2008) 020.
[105] T. Clemson, K. Koyama, G. B. Zhao, R. Maartens, and J. Valiviita, Interacting dark energy–Constraints and degeneracies, Phys. Rev. D **85**, 043007 (2012).
[106] R. Adam *et al.* (Planck Collaboration), Planck 2015 results. I. Overview of products and scientific results, Astron. Astrophys. **594**, A1 (2016).
[107] N. Aghanim *et al.* (Planck Collaboration), Planck 2015 results. XI. CMB power spectra, likelihoods, and robustness of parameters, Astron. Astrophys. **594**, A11 (2016).
[108] M. Betoule *et al.* (SDSS Collaboration), Improved cosmological constraints from a joint analysis of the SDSS-II and SNLS supernova samples, Astron. Astrophys. **568**, A22 (2014).
[109] F. Beutler, C. Blake, M. Colless, D. H. Jones, L. Staveley-Smith, L. Campbell, Q. Parker, W. Saunders, and F. Watson, The 6dF Galaxy survey: Baryon acoustic oscillations and the local Hubble constant, Mon. Not. R. Astron. Soc. **416**, 3017 (2011).
[110] A. J. Ross, L. Samushia, C. Howlett, W. J. Percival, A. Burden, and M. Manera, The clustering of the SDSS DR7 main Galaxy sample I. A 4 per cent distance measure at $z = 0.15$, Mon. Not. R. Astron. Soc. **449**, 835 (2015).
[111] H. Gil-Marín *et al.*, The clustering of galaxies in the SDSS-III Baryon oscillation spectroscopic survey: BAO measurement from the LOS-dependent power spectrum of DR12 BOSS galaxies, Mon. Not. R. Astron. Soc. **460**, 4210 (2016).
[112] M. Moresco, L. Pozzetti, A. Cimatti, R. Jimenez, C. Maraston, L. Verde, D. Thomas, A. Citro, R. Tojeiro, and D. Wilkinson, A 6% measurement of the Hubble parameter at $z \sim 0.45$: Direct evidence of the epoch of cosmic re-acceleration, J. Cosmol. Astropart. Phys. 05 (2016) 014.
[113] A. G. Riess, S. Casertano, W. Yuan, L. M. Macri, and D. Scolnic, Large magellanic cloud cepheid standards provide

a 1% foundation for the determination of the Hubble constant and stronger evidence for physics beyond LambdaCDM, Astrophys. J. **876**, 85 (2019).

[114] A. Lewis and S. Bridle, Cosmological parameters from CMB and other data: A Monte Carlo approach, Phys. Rev. D **66**, 103511 (2002).

[115] A. Lewis, A. Challinor, and A. Lasenby, Efficient computation of CMB anisotropies in closed FRW models, Astrophys. J. **538**, 473 (2000).

[116] N. Aghanim *et al.* (Planck Collaboration), Planck 2018 results. VI. Cosmological parameters, arXiv:1807.06209.

[117] P. A. R. Ade *et al.* (Planck Collaboration), Planck 2015 results. XIII. Cosmological parameters, Astron. Astrophys. **594**, A13 (2016).

[118] A. G. Riess *et al.*, A 2.4% determination of the local value of the Hubble constant, Astrophys. J. **826**, 56 (2016).

[119] A. G. Riess *et al.*, New parallaxes of Galactic cepheids from spatially scanning the Hubble space telescope: Implications for the Hubble constant, Astrophys. J. **855**, 136 (2018).

[120] A. Heavens, Y. Fantaye, A. Mootoovaloo, H. Eggers, Z. Hosenie, S. Kroon, and E. Sellentin, Marginal likelihoods from Monte Carlo Markov chains, arXiv:1704.03472.

[121] A. Heavens, Y. Fantaye, E. Sellentin, H. Eggers, Z. Hosenie, S. Kroon, and A. Mootoovaloo, No Evidence for Extensions to the Standard Cosmological Model, Phys. Rev. Lett. **119**, 101301 (2017).

[122] R. E. Kass and A. E. Raftery, Bayes factors, J. Am. Stat. Assoc. **90**, 773 (1995).